COMBINATION THERAPY FOR CANCER WITH IL-27 AND ANTI-PD-1: A SIMPLIFIED MATHEMATICAL MODEL

KENTON D. WATT AND KANG-LING LIAO

ABSTRACT. Many experiential and clinical trials in cancer treatments show that a combination of immune checkpoint inhibitors with another agent can improve the tumor reduction. Anti-Programmed death 1 (Anti-PD-1) is one of these immune checkpoint inhibitors that re-activates immune cells to inhibit the tumor growth. In this work, we consider a combination treatment of anti-PD-1 and Interleukin-27 (IL-27). IL-27 has anti-tumor functions to promote the development of Th1 and CD8$^+$ T cells, but it also upregulates the expression of PD-1 and Programmed death ligand 1 (PD-L1) to inactivate these T cells. Thus, the functions of IL-27 in tumor growth is controversial. Hence, we create a simplified mathematical model to investigate whether IL-27 is pro-tumor or anti-tumor in the combination with anti-PD-1 and to what degree anti-PD-1 improves the efficacy of IL-27. Our synergy analysis for the combination treatment of IL-27 and anti-PD-1 shows that (i) anti-PD-1 can efficiently improve the treatment efficacy of IL-27; and (ii) there exists a monotone increasing function $F_c(G)$ depending on the treatment efficacy of anti-PD-1 G such that IL-27 is an efficient anti-tumor agent when its dose is smaller than $F_c(G)$, whereas IL-27 is a pro-tumor agent when its dose is higher than $F_c(G)$. Our analysis also provides the existence and the local stability of the trivial, non-negative, and positive equilibria of the model. Combining with simulations, we discuss the effect of the IL-27 dosage on the equilibria and find that the T cells and IFN-γ could vanish and tumor cells preserve, when the production rate of T cells by IL-27 is low or the dosage of IL-27 is low.

1. INTRODUCTION

Programmed death 1 (PD-1) is an immunoinhibitory receptor. It is expressed on activated T cells, B cells, monocytes, and dendritic cells (DCs) [27]. Its ligand, programmed death ligand 1 (PD-L1), is a cell membrane protein expressed on T cells, B cells, monocytes, DCs, and tumor cells [34]. When PD-1 binds to PD-L1 to form the complex PD-1-PD-L1, the complex inhibits the cellular functions of the target immune cells and hence suppresses the immune responses and promotes tumor evasion [27]. Blocking the formation of this complex has therefore been recognized as a potentially effective anti-cancer treatment [15, 27, 32, 39]. Clinical trials have been showing that the monotherapy of immune checkpoint inhibitor for PD-1-PD-L1, anti-PD-1 or anti-PD-L1, efficiently reduces the toxicity, tumor size, and metastasis in different types of cancers [27], including melanoma, non-small-cell lung cancer, and bladder cancer [34]. However, the response rate of cancer patients for the monotherapy of anti-PD-1 or anti-PD-L1 is low [34]. Therefore, to improve the treatment efficacy, some combination treatments of anti-PD-1 or anti-PD-L1 are developed, including:

  (i) Combination with immunoregulatory cytokines: Both cytokines Interleukin-27 (IL-27) and Interferon-γ (IFN-γ) improve the T cell development and activities, but also upregulate PD-1

and PD-L1 to inactivate immune cells [1, 6, 38]. Therefore, combination of anti-PD-1 (or anti-PD-L1) and IL-27 (or IFN-γ) can reduce the amount of PD-1-PD-1 and hence promote the tumor reduction.

(ii) Combination with radiotherapy: When the immune checkpoint inhibitors reduce the immune responses, the radiotherapy can still induce local immunity resulting in local tumor cell death [36]. For instance, the long term survival rate in mice intracranial gliomas is improved by using the combination treatment of anti-PD-1 and radiotherapy [36].

(iii) Combination with vaccines: Cancer vaccines can enhance anti-tumor immune response via increasing the population and activity of the tumor-specific T cells [22]. For instance, preclinical studies in B16 melanoma shows that combination of the cancer vaccine GVAX and anti-PD-1 improves the survival rate [36].

(iv) Combination with oncolytic virus (OV): When cancer cells are infected by the OV, the virus infected cancer cells trigger immune responses to attract more cytotoxic T cells and macrophages resulting in efficient cancer cells eradication [11]. However, the cancer cells eradication could be diminished by the innate immune cells, such as macrophages [11]. Thus, combination with immune checkpoint inhibitors to reduce the activity of innate immune cells could be an option to improve the treatment efficacy of OV [36].

Some Partial Differential Equations (PDEs) models are developed to investigate these combination therapies with checkpoint inhibitors [11, 22, 23, 26]. The cancer vaccine GVAX induces the production of Granulocyte-macrophage colony stimulating factor (GM-CSF) to activate DCs and then recruit more T cells which can maintain their activity by anti-PD-1. In [22], the positively correlation between the anti-PD-1 and GVAX vaccine to the tumor volume was found. In [23], the authors investigated the combination treatment of anti-PD-1 and BRAF/MEK inhibitor for melanoma treatment. Their simulation indicated that, the tumor volume decreased as one of the dosages increased within a low dosage region, whereas the tumor volume increased as one of the dosages increased within a large dosage region. A similar result that the two treatments were antagonistic for such ranges of doses was obtained when considering the combination of anti-PD-1 and OV in [11]. In [24], the authors investigated the combination therapy of the radiation therapy (RT) and anti-PD-1 and compared the treatment efficacy based on the treatment agent administration order and schedule. In [26], the authors generated a mathematical model including the pro-inflammatory and anti-inflammatory functions of IFN-γ to investigate the tumor growth under anti-PD-1 treatment in the wild type and IFN-γ knockdown and over-expression mutants in melanoma.

In this paper we address the question by a mathematical model: to what degree the anti-PD-1 improves the treatment efficacy of immunoregulatory cytokines. We consider a special case where the anti-PD-1 combines with the immunotherapeutic drug IL-27, but the methodology developed here could also be applied to other immunoregulatory cytokines, such as IFN-γ.

IL-27 mediates anti-tumor activities through several mechanisms including direct inhibition of growth, proliferation, and migration of cancer cells [7], enhancement of NK T cell activity [31], and promotion of Th1 cells [18] and CD8$^+$ T cells [33] activation. IL-27 also promotes the production of IL-10 by CD8$^+$ T cells, thereby slows down T cell apoptosis and reduces tumor volume [28]. Additionally, IL-27 inhibits IL-2 production by Th1 and CD8$^+$ T cells [37], which limits the activation of regulatory T cells (T$_{reg}$s) [17, 37], Th1, and CD8$^+$ T cells [4, 20]. IL-27 also promotes B cells to produce more antibodies [19]. On the other hand, IL-27 also induces pro-tumor activities. For instance, IL-27 has been shown to induce the expression of PD-1 and PD-L1 in T cells [5, 16], which in turn induces the tolerance in T cells [35] and promotes tumor metastasis [14] by interacting with PD-L1 on tumor cells [16, 35]. Moreover, IL-27 inhibits the development and immune responses of Th17 cells [19] and the production of IFN-γ

in plasmacytoma [28]. Thus, whether IL-27 is an anti-tumor or pro-tumor agent is still a controversial issue [10]. In this paper we address this controversy in the context of combination therapy of IL-27 with anti-PD-1.

It was demonstrated by Liu et al. in [28] that IL-27 increased the population of cytotoxic T lymphocytes (CTLs), promoted the production of IL-10 to prolong the survival of $CD8^+$ T cells, and inhibited the production of IFN-γ by Th1 and $CD8^+$ T cells, resulting in tumor reduction in plasmacytoma. Although IL-27 has both pro-inflammatory and anti-inflammatory functions, the overall outcome of IL-27 in plasmacytoma is still tumor reduction. In [12, 25], the authors provided PDE models including the effect of CTLs, IL-10, $CD8^+$ T cells, and IFN-γ from IL-27 to capture the experimental data from plasmacytoma shown in [28]. Their simulations showed that the tumor reduction increased as the production rate of IL-27 increased, suggesting that IL-27 was an efficient drug in the considered dosage in plasmacytoma. In [38], Zhu et al. further investigated the combination treatment of IL-27 and anti-PD-1 in B16F10 melanoma. In their experiments, the melanoma cells were injected into mice and the tumor volume was measured every 2 or 3 days. For the IL-27 treatment, four days after the tumor engraftment, the AAV-IL-27 virus was injected into mice once to make muscle cells persistently produce a high level of IL-27 resulting in a constant level of IL-27 in blood after day 5 (Fig 1A in [38]). For the anti-PD-1 treatment, each mouse was injected with $300\mu g$ of anti-PD-1 at 3-day intervals for up to 3 to 4 times during the experiment. Under this experimental setting, the experimental results in Fig 7D in [38] showed that there was no significant difference of tumor volume between the control case and monotherapy of anti-PD-1 during the whole treatment, the monotherapy of IL-27 significantly reduced the tumor volume, and the tumor growth was totally suppressed when both IL-27 and anti-PD-1 were applied. Hence, in melanoma, IL-27 still acts as an efficient treatment agent and the PD-1 blockade by anti-PD-1 dramatically enhances the efficacy of IL-27 therapy.

In this work, based on the melanoma experiments in mice from [38], we construct a simplified Ordinary Differential Equations (ODEs) model that includes the tumor cells, T cells, and IFN-γ measured in the experiments in [38]. We use the model to investigate the treatment efficacy of IL-27 and anti-PD-1 in melanoma, using different dosage of IL-27 (I_{27}) and the treatment efficacy of anti-PD-1 (G) and to study the following questions. (i) To what degree anti-PD-1 improves the efficacy of immunotherapeutic drugs? (ii) Whether IL-27 is pro-tumor or anti-tumor in the combination with anti-PD-1?

Our simulation shows that IL-27 acts like an anti-tumor cytokine when the dosage is low, whereas it acts like a pro-tumor cytokine when the dosage is high. Moreover, for the combination therapy of IL-27 and anti-PD-1, we have the following nonlinear treatment result:
(i) Increasing anti-PD-1 can rapidly increase the tumor reduction, under any fixed IL-27 dosage. This finding displays the degree of anti-PD-1 improving the efficacy of the immunotherapeutic drug IL-27.
(ii) There exists a monotone increasing function, $F_c(G)$, depending on the treatment efficacy of anti-PD-1 (G), such that (ii-a) If $I_{27} < F_c(G)$, then tumor reduction increases as the dosage of IL-27 increases suggesting that IL-27 acts like a potent anti-tumor cytokine in this regime. (ii-b) If $I_{27} > F_c(G)$, then tumor reduction decreases as the dosage of IL-27 increases suggesting that the treatment efficacy of IL-27 is reduced and IL-27 acts like a pro-tumor cytokine in this regime. This finding shows the balance between the anti-tumor and pro-tumor functions of IL-27. Under a small dosage of IL-27, the anti-PD-1 efficiently binds to the free PD-1 and hence reduces the formation of PD-1-PD-L1 produced by IL-27 such that the increased T cells can be activated to kill tumor cells. However, under a high dosage of IL-27, the PD-1 and PD-L1 are dramatically increased by IL-27 resulting in a large amount of PD-1-PD-L1. Therefore, the same amount of anti-PD-1 cannot efficiently reduce the amount of PD-1-PD-L1, and the remained PD-1-PD-L1 still can effectively deactivate T cells and reduce the treatment efficacy of

IL-27. Therefore, in combination with anti-PD-1, the drug IL-27 is effective in reducing tumor volume only if given in a small dose (i.e., smaller than $F_c(G)$).

We also perform local sensitivity analysis to investigate how the parameters affect the transient behavior of tumor cells, T cells, and IFN-γ, when the dosage of IL-27 and the treatment efficacy of anti-PD-1 are at different levels. We then use the global sensitivity analysis to further study how the parameter values affect the tumor cell density ratio of the combination treatment to the control case. Next, we analyze the basic dynamics of the model to obtain the positive invariant set, as well as the existence and the local stability of the trivial, non-negative, and positive equilibria. We then provide a numerical example to study the effect of the IL-27 dosage on the number and stability of all equilibria.

This paper is organized as follows. In Section 2, we introduce the ODE model. In the Section 3, we display the numerical simulations to generate the anti-tumor and pro-tumor reactions of IL-27, and the synergy analysis between the IL-27 and anti-PD-1 on tumor growth. The local and global sensitivity analyses are performed in the Section 4. In Section 5, we analyze the basic dynamics of the model and provide one numerical example to investigate how the IL-27 dosage affects the number and stability of the equilibria. The paper ends with a discussion in Section 6.

2. Results

2.1. **Mathematical Model.** We constructed a system of ODEs based on the system network shown in Fig. 1. The variables of the model are as follows:

$C(t)$: Density of tumor cells at time t with unit g/cm^3,

$T(t)$: Density of T cells, including CTLs, Th1, and CD8$^+$ T cells at time t with unit g/cm^3,

$I_\gamma(t)$: Concentration of Interferon-γ (IFN-γ) at time t with unit g/cm^3.

The parameter values are listed in Table 1 and the parameter estimation is shown in the Methods section. The following is the explanation of each equation of the model.

TABLE 1. **Parameters of the model**

| Parameter	Description	Value	Reference
λ_{TC}	Production rate of T cells by immune response	$6 \times 10^{-3}/day$	[11, 25, 38] & estimated
λ_{TI_γ}	Production rate of T cells by IFN-γ	$0.6/day$	[11, 25, 38] & estimated
$\lambda_{TI_{27}}$	Production rate of T cells by IL-27	$0.1755/day$	[11, 38] & estimated
$\lambda_{I_\gamma T}$	Production rate of IFN-γ by T cells	$1.656 \times 10^{-7}/day$	[11, 28] & estimated
λ_C	Growth rate of Tumor cells	$1.416/day$	[11, 25, 38] & estimated
k_{27}	Half-saturation of IL-27	$1.1 \times 10^{-6}\ g/cm^3$	[38]
k_C	Half-saturation of tumor cells	$0.4965\ g/cm^3$	[11]
k_γ	Half-saturation of IFN-γ	$4.5 \times 10^{-11}\ g/cm^3$	[28]
s_γ	Inhibition saturation of IL-27 for IFN-γ	$4.4 \times 10^{-6}\ g/cm^3$	[38] & estimated
k_q	Half-saturation of IL-27	$1.1 \times 10^{-6}\ g/cm^3$	[38]
μ_T	Death rate of T cells	$0.3/day$	[25]
μ_C	Death rate of Tumor cells	$0.173/day$	[25]
μ_γ	Degradation rate of IFN-γ	$3.68/day$	[2]
I_{27}	I_{27} amount for anti-tumor result	$1.1 \times 10^{-6}\ g/cm^3$	[38]
I_{27}	I_{27} amount for pro-tumor result	$5.5 \times 10^{-6}\ g/cm^3$	[38] & estimated
G	Efficacy of anti-PD-1 drug	0.1	estimated
V_{max}	Maximal production rate of PD-1-PD-L1 by IL-27	0.24	estimated
Q_0	Amount of PD-1-PD-L1 without IL-27	0.01	estimated
C_M	Carrying capacity of Tumor cells	$0.9\ g/cm^3$	[9]
η_C	Killing rate of Tumor cells by T cells	$231\ cm^3/g/day$	[11, 38] & estimated
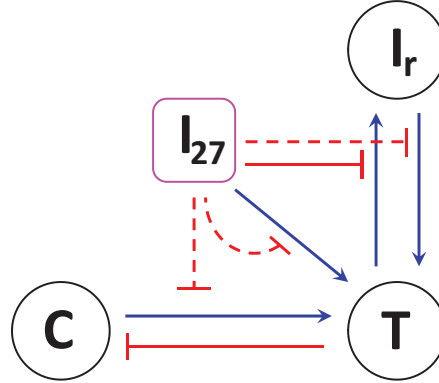
FIGURE 1. **The system network.** Tumor cells trigger the immune responses that attract T cells to kill tumor cells. T cells produce IFN-γ, and IFN-γ promotes the production and activation of T cells. IL-27 promotes the activation of T cells and inhibits the production of IFN-γ by T cells. The PD-1-PD-L1 inhibits the activation of T cells and IL-27 promotes the expression of PD-1 and PD-L1 resulting in an increased amount of PD-1-PD-L1. Thus, the increased PD-1-PD-L1 by IL-27 inhibits the immune responses of T cells by tumor cells and the production of T cells by IFN-γ and by IL-27, which are shown by the dashed non-arrow lines and curves. The formation of PD-1-PD-L1 is inhibited by anti-PD-1 (G), due to the binding between anti-PD-1 and free PD-1. Thus, the reactions shown by the dashed non-arrow lines are suppressed by the anti-PD-1. The arrows represent the promotion reaction and the non-arrow lines represent the inhibition reaction.

Tumor Cells $(C(t))$

The density of tumor cells satisfies the following equation:

$$\frac{dC}{dt} \;=\; \underbrace{\lambda_C C \left(1 - \frac{C}{C_M}\right)}_{\text{Growth}} - \underbrace{\eta_C T C}_{\text{Death by T cells}} - \underbrace{\mu_C C}_{\text{Death}}. \tag{2.1}$$

The first term represents the logistic growth of the tumor cells, with carrying capacity C_M. The second and last terms represent the killing of tumor cells by T cells and the natural death of tumor cells, respectively.

T cells $(T(t))$

The equation for the T cell density is as follows:

$$\frac{dT}{dt} = \left(\underbrace{\lambda_{TC} T \frac{C}{C + k_C}}_{\text{immune response}} + \underbrace{\lambda_{TI_\gamma} T \frac{I_\gamma}{I_\gamma + k_\gamma}}_{\text{promotion by IFN-}\gamma} + \underbrace{\lambda_{TI_{27}} T \frac{I_{27}}{I_{27} + k_{27}}}_{\text{promotion IL-27}} \right) \times \underbrace{\frac{1}{1 + Q(I_{27}) \times (1 - G)}}_{\text{inhibition by PD-1-PD-L1}}$$
$$- \underbrace{\mu_T T}_{\text{death}}. \tag{2.2}$$

The first term represents the (indirect) activation of T cells by the immune response triggered by the tumor cells. The second and third terms represent the promotion of T cells by IFN-γ and IL-27 [38], respectively. The first three terms for T cell reactions are inhibited by the PD-1-PD-L1 complex shown

by the factor $1/(1 + Q(I_{27}) \times (1 - G))$. Notice that, in [38], the AAV-IL-27 virus was injected into mice once to make muscle cells persistently produce a high level of IL-27 resulting in a constant level of IL-27 in blood (Fig 1A in [38]), so we use a parameter I_{27} to represent the constant concentration of IL-27 in blood. PD-1 is expressed by T cells, and PD-L1 is expressed by T cells and cancer cells. Moreover, IL-27 promotes the expression of PD-1 and PD-L1 by T cells resulting in a significant increase of PD-1-PD-L1 [5, 16]. Thus, for simplicity, we assume that the variation of PD-1-PD-L1 amount is mainly controlled by the concentration of IL-27 and the amount of PD-1-PD-L1 produced by T cells and cancer cells is close to a constant Q_0. Then we use the following function $Q(I_{27})$ to represent the total amount of PD-1-PD-L1

$$Q(I_{27}) = \frac{V_{max} I_{27}}{k_q + I_{27}} + Q_0. \tag{2.3}$$

The first term in Eq. (2.3) represents the increase of PD-1-PD-L1 by IL-27 which is shown by the Michaelis-Menten type with the maximal rate V_{max} and Michaelis constant k_q. The second term in Eq. (2.3), Q_0, is the baseline amount of PD-1-PD-L1 produced by T cells and cancer cells. The anti-PD-1 binds to the free PD-1 and hence reduces the formation of PD-1-PD-L1 resulting in a fewer amount of PD-1-PD-L1. Thus, for simplicity, we use the constant G in Eq. (2.2) to represent the indirect effect on PD-1-PD-L1 by anti-PD-1, namely, the reduction of PD-1-PD-L1 is caused by the reduced free PD-1 by anti-PD-1, and call G is the efficacy of the drug anti-PD-1. Hence, $G = 0$ represents no reduction of PD-1-PD-L1 and $G = 1$ represents a complete reduction of PD-1-PD-L1. The last term in the right-hand side of Eq. (2.2) represents the natural death of T cells.

IFN-γ $(I_\gamma(t))$
The dynamics of the concentration of IFN-γ satisfies the following equation:

$$\frac{dI_\gamma}{dt} = \underbrace{\lambda_{I_\gamma T} T \frac{s_\gamma}{s_\gamma + I_{27}}}_{\text{Production by T cells}} - \underbrace{\mu_\gamma I_\gamma}_{\text{Decay}}. \tag{2.4}$$

The first term represents the production of IFN-γ by T cells which is inhibited by IL-27 [28]. The factor $\lambda_{I_\gamma T} T$ is the normal production of IFN-γ by T cells with the production rate $\lambda_{I_\gamma T}$. For simplicity, we use the decreasing function of I_{27}, $\frac{s_\gamma}{s_\gamma + I_{27}}$, to represent the inhibition by IL-27. The last term is the degradation of IFN-γ.

Initial Conditions
Since the carrying capacity of the tumor cells is around 10^9 $cell/cm^3 \approx 1$ g/cm^3 and we assume that the model starts from the tumor initiation, so we take $C(0) = 0.4965$ g/cm^3. We take the initial values of T and I_γ to be their steady state values. The steady states are estimated in the Methods section. Thus,

$$C(0) = 0.4965 \ g/cm^3, \ T(0) = 1 \times 10^{-3} \ g/cm^3, \ I_\gamma(0) = 4.5 \times 10^{-11} \ g/cm^3.$$

Notice that different initial conditions with appropriate value of I_{27} will not change the model dynamics significantly.

Non-dimensionalization

We non-dimensionalizate the variables and parameters using the following formulas:

$$\hat{C} = C/C_0, \ \hat{T} = T/T_0, \ \hat{I}_\gamma = I_\gamma/I_\gamma^0, \ \hat{t} = t/\tau,$$

$$\{\hat{\lambda}_{TC}, \ \hat{\lambda}_{TI_\gamma}, \ \hat{\lambda}_{TI_{27}}, \ \hat{\lambda}_{I_\gamma T}, \ \hat{\lambda}_C\} = \tau\{\lambda_{TC}, \ \lambda_{TI_\gamma}, \ \lambda_{TI_{27}}, \ \lambda_{I_\gamma T}, \ \lambda_C\},$$

$$\{\hat{k}_{27}, \ \hat{k}_C, \ \hat{C}_M, \ \hat{k}_\gamma, \ \hat{s}_\gamma, \ \hat{k}_q, \ \hat{I}_{27}\} = \{k_{27}/I_{27}^0, \ k_C/C_0, C_M/C_0, \ k_\gamma/I_\gamma^0, \ s_\gamma/I_{27}^0, \ k_q/I_{27}^0, \ I_{27}/I_{27}^0\},$$

$$\{\hat{\mu}_T, \ \hat{\mu}_C, \ \hat{\mu}_\gamma\} = \tau\{\mu_T, \ \mu_C, \ \mu_\gamma\}, \ \hat{\eta}_C = \tau T_0 \eta_C, \ \hat{V}_{max} = V_{max}, \ \hat{Q}_0 = Q_0,$$

with

$$C_0 = 0.4965 \ g/cm^3, \ T_0 = 10^{-3} \ g/cm^3, \ I_\gamma = 4.5 \times 10^{-11} \ g/cm^3, \ \tau = 3 \ days, \ I_{27}^0 = 1.1 \times 10^{-6} \ g/cm^3.$$

All simulations are performed with non-dimensionalized parameters and variables. Below is the system of non-dimensional equations, dropping the " ˆ " for simplicity:

$$\begin{cases} \dfrac{dC}{dt} = \underbrace{\lambda_C C \left(1 - \dfrac{C}{C_M}\right)}_{\text{Growth}} - \underbrace{\eta_C TC}_{\text{Death by T cells}} - \underbrace{\mu_C C}_{\text{Death}} \\[4mm] \dfrac{dT}{dt} = \left(\underbrace{\lambda_{TC} T \dfrac{C}{C + k_C}}_{\text{Immune Response}} + \underbrace{\lambda_{TI_\gamma} T \dfrac{I_\gamma}{I_\gamma + k_\gamma}}_{\text{Production by IFN-}\gamma} + \underbrace{\lambda_{TI_{27}} T \dfrac{I_{27}}{I_{27} + k_{27}}}_{\text{Production by IL-27}}\right) \times \underbrace{\dfrac{1}{1 + Q(I_{27}) \times (1 - G)}}_{\text{Inhibition by PD-1-PD-L1 Complex}} \\[4mm] \qquad - \underbrace{\mu_T T}_{\text{Death}} \\[4mm] \dfrac{dI_\gamma}{dt} = \underbrace{\lambda_{I_\gamma T} T \dfrac{s_\gamma}{s_\gamma + I_{27}}}_{\text{Production by T cells}} - \underbrace{\mu_\gamma I_\gamma}_{\text{Decay}}. \end{cases} \quad (2.5)$$

3. Numerical Simulation

In this section, we use the model (2.5) to investigate the functions of IL-27 in tumor growth and the efficacy of combination of IL-27 and anti-PD-1 in cancer treatment. We first display that the functions of IL-27 switches from anti-tumor agent to pro-tumor agent as its dosage increases in the subsection 3.1. We then use the synergy analysis to investigate: (i) whether IL-27 is pro-tumor or anti-tumor in the combination with anti-PD-1, and (ii) to what degree anti-PD-1 improves the efficacy of IL-27 in the subsection 3.2. The ode45 package in MatLab was used to generate the simulation results in the subsection 3.1 and the backwards Euler method was used with step size $dt = 0.003$ *days* in the subsection 3.2.

3.1. **Anti-Tumor versus Pro-Tumor Results.** IL-27 has both anti-tumor functions including promotion of T cell development and pro-tumor functions including upregulation of PD-1 and PD-L1 and inhibition of IFN-γ in the tumor microenvironment (TME). Hence, we hypothesize that whether IL-27 acts more like an anti-tumor or pro-tumor agent depends on the balance between its anti-tumor and pro-tumor functions. We also hypothesize that when the dosage of IL-27 is relatively small, the upregulated PD-1 and PD-L1 by IL-27 cannot efficiently inactivate T cells resulting in tumor reduction. However, when the dosage of IL-27 is relatively large, then the PD-1 and PD-L1 are dramatically increased by IL-27 and then inactivate most T cells resulting in tumor promotion.

To verify our hypotheses and to investigate the interaction between IL-27 and anti-PD-1, we consider the following four cases under different dosages of IL-27 (I_{27}):

(i) Ctrl-IL27/Ctrl-Ab: there is neither IL-27 nor anti-PD-1, i.e., $I_{27} = 0$ and $G = 0$;
(ii) Ctrl-IL27/Ab: there is anti-PD-1, but no IL-27, i.e., $I_{27} = 0$ and $0 < G \leq 1$;
(iii) IL27/Ctrl-Ab: there is IL-27, but no anti-PD-1, i.e., $I_{27} > 0$ and $G = 0$;
(iv) IL27/Ab: there is IL-27 and anti-PD-1, i.e., $I_{27} > 0$ and $0 < G \leq 1$.

The injected dosage of IL-27 in [38] is $f_0 := 1.1 \times 10^{-6}$ g/cm^3, so we set f_0 to be the baseline of the IL-27 dosage. Fig. 2 shows the simulation results of model (2.5) for cases (i)-(iv) under a small dosage of IL-27, i.e., $I_{27} = f_0 = 1.1 \times 10^{-6}$ g/cm^3, while Fig. 3 displays the model outcomes of cases (i)-(iv) under a large dosage of IL-27, i.e., $I_{27} = 5f_0 = 5.5 \times 10^{-6}$ g/cm^3.

In Fig. 2, when considering a small dosage f_0 of IL-27, we have the following finding:
(I-i) The monotherapy of anti-PD-1 (i.e., case (ii)) only slightly reduces the tumor cell density, and slightly increases the density of T cells and the concentration of IFN-γ;
(I-ii) The monotherapy of IL-27 (i.e., case (iii)) induces a significant tumor reduction, and significantly increases the density of T cells and the concentration of IFN-γ; and
(I-iii) The best tumor reduction and the highest T cell density and IFN-γ concentration are obtained when applying both anti-PD-1 and IL-27 (i.e., case (iv)).
Thus, the monotherapy of anti-PD-1 is not an efficient treatment method. Moreover, a small amount of IL-27 can still efficiently increase the density of T cells resulting in tumor reduction, even though the production of IFN-γ of each T cell is reduced by IL-27. This result suggests that IL-27 is more like an anti-tumor cytokine at a small dosage. Additionally, combination of IL-27 and anti-PD-1 improves the treatment efficacy of both IL-27 and anti-PD-1.
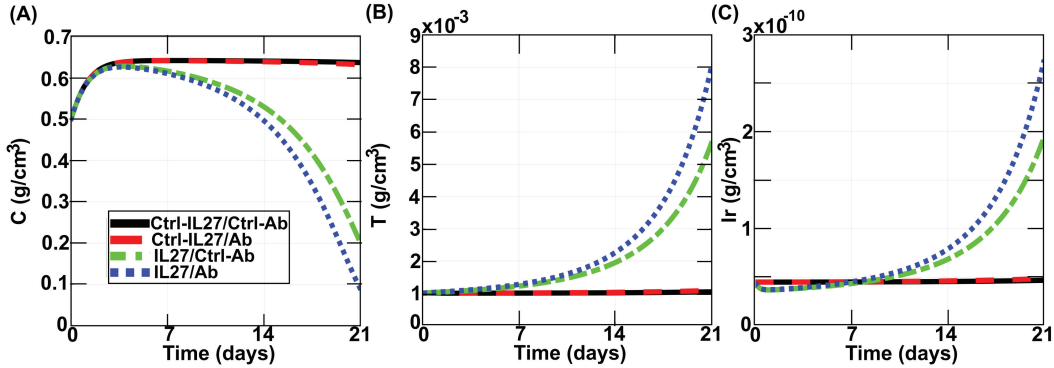

FIGURE 2. **Dynamics of the model** (2.5) **under a low dose of IL-27.** (A)-(C) show the dynamics of tumor cells, T cells, and IFN-γ of cases (i)-(iv) with the dosage of IL-27 $f_0 = 1.1 \times 10^{-6}$ g/cm^3, respectively. The black solid, red dashed, green dashed-dotted, and the blue dotted curves represent the cases (i) Ctrl-IL27/Ctrl-Ab, (ii) Ctrl-IL27/Ab, (iii) IL27/Ctrl-Ab, and (iv) IL27/Ab, respectively. The horizontal axis and vertical axis represent the time with unit days and the density of each variable with unit g/cm^3, respectively.

On the other hand, in Fig. 3, when considering a large dosage of IL-27, i.e., $I_{27} = 5f_0$, we have the following conclusion:
(II-i) The dynamics of tumor cells, T cells, and IFN-γ in the monotherapy of anti-PD-1 (i.e., case (ii)) are the same as the one in (I-i);
(II-ii) The fastest tumor growth and the lowest T cell density and IFN-γ concentration appear when applying IL-27 alone (i.e., case (iii)).

(II-iii) When considering the combination of IL-27 and anti-PD-1 (i.e., case (iv)), the increased tumor cell density by IL-27 is reduced slightly by anti-PD-1, as well as the reduced T cell density and IFN-γ concentration by IL-27 are restored slightly by anti-PD-1.

Although a large dosage of IL-27 increases the density of T cells, it also induces plenty of PD-1-PD-L1 complex to inactivate the increased T cells and hence reduces the density of (activated) T cells and promotes the tumor growth. When applying a large dosage of IL-27 with anti-PD-1, the amount of anti-PD-1 cannot efficiently reduce the amount of PD-1-PD-L1 complex, so anti-PD-1 can only reduce the tumor growth slightly. Thus, a large dose of IL-27 shifts the IL-27 from an anti-tumor agent to a pro-tumor agent. Moreover, the efficacy of anti-PD-1 reduces as the amount of IL-27 increases.

Combining the findings of Figs. 2 and 3, the dosage of IL-27 determines the functions of IL-27 in tumor growth and the treatment efficacy of anti-PD-1. Under a small dosage of IL-27, IL-27 acts more like an anti-tumor agent and the anti-PD-1 can efficiently improve the treatment efficacy of IL-27. On the other hand, under a large dosage of IL-27, IL-27 acts more like a pro-tumor agent and the anti-PD-1 cannot efficiently improve the treatment efficacy of IL-27.
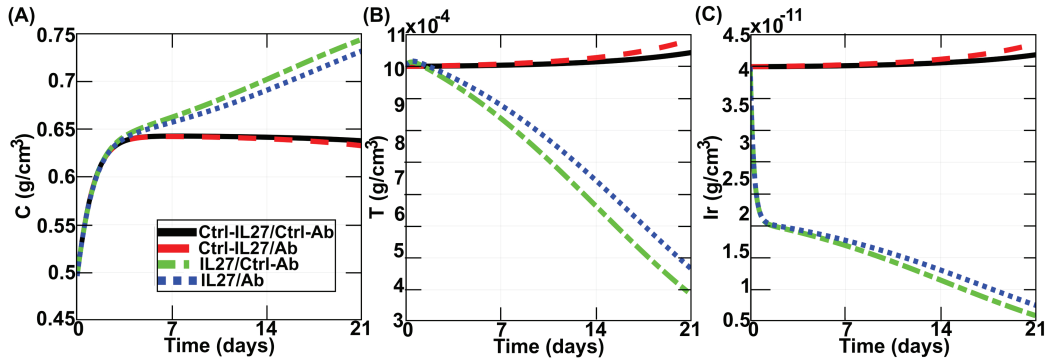

FIGURE 3. **Dynamics of the model** (2.5) **under a high dose of IL-27.** (A)-(C) show the dynamics of tumor cells, T cells, and IFN-γ of cases (i)-(iv) with the dosage of IL-27 $5f_0 = 5.5 \times 10^{-6}$ g/cm^3, respectively. The black solid, red dashed, green dashed-dotted, and the blue dotted curves represent the case (i) Ctrl-IL27/Ctrl-Ab, (ii) Ctrl-IL27/Ab, (iii) IL27/Ctrl-Ab, and (iv) IL27/Ab, respectively. The horizontal axis and vertical axis account for the time with unit days and the density of each variable with unit g/cm^3, respectively.

3.2. **Synergy Analysis.** In this section, we further analyze how the dose of IL-27 (I_{27}) and the treatment efficacy of anti-PD-1 (G) affect the tumor cell density by using the synergy analysis. We take $I_{27} \in [0, 5f_0] = [0, 5.5] \times 10^{-6}$ g/cm^3 and equally divide this interval into 251 points. We also take $G \in [0, 0.4]$ and equally divide this interval into 41 points. For each fixed I_{27} and G, we measure the ratio of the tumor cell density

$$R(I_{27}, G) = C^+(t)/C^-(t) \text{ at } t = 21 \text{ } days, \tag{3.1}$$

where $C^+(t)$ represents the tumor cell density at time t under the dose of IL-27 (I_{27}) and the treatment efficacy of anti-PD-1 (G), and $C^-(t)$ represents the tumor cell density at time t without any treatment. Thus, $R(I_{27}, G) < 1$ shows that the treatment under the dosage (I_{27}, G) decreases the tumor cell density, whereas $R(I_{27}, G) > 1$ shows that the tumor cell density increases under the dosage (I_{27}, G).

The heat map of $R(I_{27}, G)$ shown in Fig. 4 provides the following conclusion:

(i) Increasing G always increases the reduction of tumor cell density. In fact, the tumor cell density ratio $R(I_{27}, G)$ in Fig. 4 can be reduced from 1 to 0.2 by increasing the efficacy of anti-PD-1 (G), under appropriate dosage of IL-27 (i.e., around $3f_0$). This result suggests that the anti-PD-1 is an efficient anti-tumor agent in this regime and displays the degree of anti-PD-1 improving the efficacy of IL-27.

(ii) There exists a monotone increasing curve, $F_c(G)$ depending on G (namely, the solid pink curve in Fig. 4) dividing the $R(I_{27}, G)$ plane into two regions, such that the following holds:

(ii-a) If $I_{27} < F_c(G)$, then increasing I_{27} increases the reduction of tumor cell density which means that the anti-tumor functions are stronger than the pro-tumor functions of IL-27, under the effect of anti-PD-1. Thus, IL-27 is an efficient anti-tumor agent and the treatment efficacy increases as I_{27} increases, in this regime.

(ii-b) If $I_{27} > F_c(G)$, then increasing I_{27} decreases the reduction of tumor cell density, which means that the pro-tumor functions of IL-27 are getting stronger as I_{27} increases, under the effect of anti-PD-1. Hence, IL-27 is more like a pro-tumor agent and the treatment efficacy decreases as I_{27} increases, in this regime.

The above finding clarifies the controversy of IL-27 by showing the balance between the anti-tumor and pro-tumor functions of IL-27, under the presence of anti-PD-1. Under a small dosage of IL-27 $(I_{27} < F_c(G))$, the anti-PD-1 can efficiently reduce the amount of the PD-1-PD-L1 (indirectly) produced by IL-27 such that the increased T cells can be activated to kill tumor cells. However, under a high dosage of IL-27 $(I_{27} > F_c(G))$, the PD-1-PD-1 is dramatically increased by IL-27 such that the same amount of anti-PD-1 cannot efficiently reduce the amount of the PD-1-PD-L1 resulting in deactivation of T cells and reduced treatment efficacy of IL-27. Therefore, the critical curve $F_c(G)$ could be used to determine the optimal dosages of IL-27 and anti-PD-1 to achieve the best tumor reduction. Thus, we conclude that, in combination with anti-PD-1, IL-27 acts as an efficient anti-tumor drug in the region $\{I_{27} < F_c(G)\}$, whereas IL-27 acts like a pro-tumor drug in the region $\{I_{27} > F_c(G)\}$.

4. Sensitivity Analysis

In this section, we perform the local and global sensitivity analysis on the model (2.5) to investigate how the parameter values affect the model dynamics. The local sensitivity analysis is used to investigate how the small change of each parameter affects the model dynamics at any time point when other parameter values are fixed, while the global sensitivity analysis is used to evaluate how the uncertainty and variations in model outputs at the selected time point are correlated to the parameter values. The drawback of the local sensitivity analysis is that we can only vary one parameter value with small changes, but this drawback can be fixed by performing the global sensitivity analysis because we can use any variation range of the selected multiple parameters in the global sensitivity analysis. On the other hand, the drawback of the global sensitivity analysis is that it can only analyze the correlation when the parameter has significant effect on the model output. This drawback can be compensated by the local sensitivity analysis because it can still analyze the effect of each parameter when the parameter does not have the significant effect on the model output. Therefore, we perform both local and global sensitivity analysis to study the relationship between the parameter values and the model output. The ode45 package in MatLab is used to generate the simulation results in this section.

4.1. **Local Sensitivity Analysis.** In this subsection, we apply the local sensitivity analysis on the model (2.5) to investigate how the parameters affect the transient behavior of variables C, T, and I_γ.

We denote the solution of the model (2.5) to be $\mathbf{X}(t) = (C(t), T(t), I_\gamma(t))^T$ and its partial derivative with respect to any parameter p to be $\mathbf{X}_p = \partial\mathbf{X}/\partial p$ with

$$p \in \{\lambda_{TC}, \lambda_{TI_\gamma}, \lambda_{TI_{27}}, \lambda_{I_\gamma T}, \lambda_C, \ k_{27}, k_C, k_\gamma, k_q, s_\gamma, \mu_C, \mu_T, \mu_\gamma, V_{max}, Q_0, C_M, \eta_C, I_{27}, G\}.$$

We then rewrite the model (2.5) as follows

$$\frac{d\mathbf{X}}{dt} = \mathbf{F}(\mathbf{X}) \text{ with } \mathbf{X}(0) = \mathbf{X}_0 = (C(0), T(0), I_\gamma(0)).$$

By applying the Chain Rule and Clairaut's Theorem, we obtain

$$\frac{d\mathbf{X}_p}{dt} = \frac{d\mathbf{F}}{d\mathbf{X}}\mathbf{X}_p + \frac{\partial\mathbf{F}}{\partial p}, \text{ with } \mathbf{X}_p(0) = \frac{\partial\mathbf{X}_0(p)}{\partial p}.$$

Therefore, we obtain the following system to perform the local sensitivity analysis of the model (2.5)

$$\begin{cases} \dfrac{d\mathbf{X}}{dt} & = & \mathbf{F}(\mathbf{X}), \ \mathbf{X}(0) = \mathbf{X}_0 \\ \dfrac{d\mathbf{X}_p}{dt} & = & \dfrac{d\mathbf{F}}{d\mathbf{X}}\mathbf{X}_p + \dfrac{\partial\mathbf{F}}{\partial p}, \ \mathbf{X}_p(0) = \dfrac{\partial\mathbf{X}_0(p)}{\partial p}. \end{cases} \tag{4.1}$$

The logarithmic sensitivity in the system (4.1) represents the percentage changes in the solution induced by positive perturbations of the paramter $p \cdot \mathbf{X}_p/\mathbf{X}$. The detailed method is provided in [3].

As shown in Fig. 4, the value of $R(I_{27}, G)$ defined as Eq. (3.1) depends heavily on the values of I_{27} and G. Thus, we perform the local sensitivity analysis based on the values of I_{27} and G, while other parameters are taken from Table 1:

(I) When the efficacy of anti-PD-1 is low (i.e., $G = 0.1$): we consider (I-i) low dose of IL-27, i.e., $I_{27} = 0.1f_0 = 1.1 \times 10^{-7} \ g/cm^3$, (I-ii) medium dose of IL-27, i.e., $I_{27} = f_0 = 1.1 \times 10^{-6} \ g/cm^3$, and
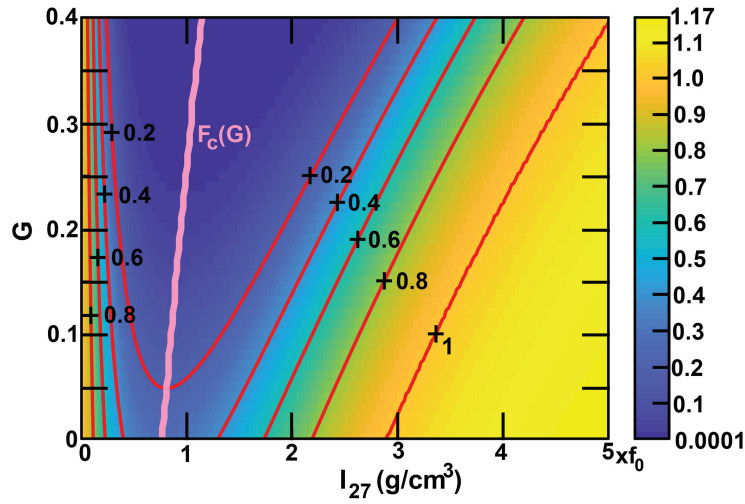

FIGURE 4. **Heat map of $R(I_{27}, G)$ for the model** (2.5). This figure shows the heat map of the tumor cell density ratio $R(I_{27}, G)$ defined as Eq. (3.1), where $I_{27} \in [0, \ 5.5 \times 10^{-6} \ g/cm^3] = [0, 5f_0]$ and $G \in [0, 0.4]$. The horizontal and vertical axes represent the values of I_{27} with unit $f_0 = 1.1 \times 10^{-6} g/cm^3$ and G, respectively. Each point represents the value $R(I_{27}, G)$ where the maximum is around 1.16628 and the minimum is around 1.3×10^{-4}. The colour bar shows the values of $R(I_{27}, G)$. The red curves represent the contours and the pink curve displays the critical curve $F_c(G)$.

(I-iii) high dose of IL-27, i.e., $I_{27} = 5f_0 = 5.5 \times 10^{-6} \ g/cm^3$.

(II) When the efficacy of anti-PD-1 is high (i.e., $G = 0.7$): we consider (II-i) low dose of IL-27, i.e., $I_{27} = 0.1f_0 = 1.1 \times 10^{-7} \ g/cm^3$, (II-ii) medium dose of IL-27, i.e., $I_{27} = f_0 = 1.1 \times 10^{-6} \ g/cm^3$, and (II-iii) high dose of IL-27, i.e., $I_{27} = 5f_0 = 5.5 \times 10^{-6} \ g/cm^3$.

The logarithmic-relative sensitivity curves $p \times X_p(t)/X(t)$ for all components with respect to the parameter p of groups (I) and (II) are displayed in Figs. 5 and 6, respectively. The sign of each parameter is listed in Table 2. The positive value (resp. negative value) of $p \times X_p(t)/X(t)$ in Figs. 5 and 6 shows that the component is positive correlated (resp. negative correlated) to the parameter p at time t, so the component increases (resp. decreases) as the parameter p increases at time t.

In Fig. 5, when I_{27} is at a low dose (case (I-i)) or a medium dose (case (I-ii)), I_{27} has negative effect on C and positive effect on T during the whole process. Moreover, I_{27} has negative effect on I_γ during $[0, 3]$ *days* at the low dose of I_{27} and during $[0, \ 18]$ *day* at the medium dose of I_{27}, and then switches to positive effect on I_γ thereafter. The zoom-in curves of I_{27} are shown in Fig 7. This result suggests that the inhibition from I_{27} on I_γ increases as the density of T cells increases induced by I_{27}. Thus, at a low or medium dose of I_{27}, IL-27 mainly promotes T cell density and inhibits tumor cell density, and hence IL-27 acts like an efficient anti-tumor drug. When I_{27} is at a high dose (i.e., case (I-iii)), I_{27} has negative effect on C during $[0, 0.35]$ *days* and then switches to positive effect on C thereafter. On the other hand, I_{27} has positive effect on T during $[0, 0.2]$ *days* and then switches to negative effect on T thereafter. Moreover, I_{27} has negative effect on I_γ during the whole process. Hence, at a high dose of I_{27}, IL-27 is still an anti-tumor agent in the early stage, but it switches to a pro-tumor agent when the IL-27 treatment is administered long enough.

Regardless of the dose of I_{27} (namely, cases (I-i)-(I-iii)), the parameters k_{27}, k_C, k_γ, μ_T, μ_γ, V_{max} and Q_0 have positive effect on C and negative effect on T and I_γ during the whole process. Increasing k_C or k_γ or k_{27} decreases the promotion of T cells. A higher value of V_{max} or Q_0 increases the value of $Q(I_{27})$ and hence decreases the T cell density. A higher value of μ_γ or μ_T reduces more T cells. Hence, all these reactions increase the tumor cell density.

On the other hand, the parameters λ_{TC}, λ_{TI_γ}, $\lambda_{TI_{27}}$, $\lambda_{I_\gamma T}$, s_γ, k_q, and G have negative effect on C and positive effect on T and I_γ during the whole process. Increasing any of λ_{TC}, λ_{TI_γ}, $\lambda_{TI_{27}}$ increases the T cell density. Similarly, T cell density increases as k_q or G increases. A higher value of $\lambda_{I_\gamma T}$ or s_γ increases the concentration of IFN-γ resulting in promoting T cell density. Hence, all these reactions decrease the tumor cell density. Additionally, the parameters λ_C and C_M have positive effect on C, T, and I_γ, whereas the parameters μ_C and η_C have negative effect on C, T, and I_γ during the whole process. Increasing the value of λ_C or C_M increases the tumor cell density which attracts more T cells. On the other hand, increasing the value of η_C or μ_C decreases the tumor cell density which induces fewer T cells. Notice that the effect of these parameters on I_γ is the same as T, due to the positive correlation between T and I_γ.

In Fig. 6, when the treatment efficacy of anti-PD-1 increases to 0.7, then the sign of $p \times X_p(t)/X(t)$ are the same as the ones shown in Fig. 5, except the effect of C_M on C at the medium dose of IL-27 (i.e., case (II-ii)). At the medium dose of IL-27, the parameter C_M has positive effect on C most of the time (i.e., during $[0, 19]$ days) and then switches to negative effect thereafter, suggesting that the tumor cell density may reach the carrying capacity C_M at the later stage. The zoom-in curves of C_M are shown in Fig 7.

4.2. **Global Sensitivity Analysis.** In this subsection, we apply the global sensitivity analysis provided in [30] to investigate how the parameter values affect the tumor cell density between the treatment case ($I_{27} > 0$ and $G > 0$) and the control case ($I_{27} = 0$ and $G = 0$) of model (2.5).
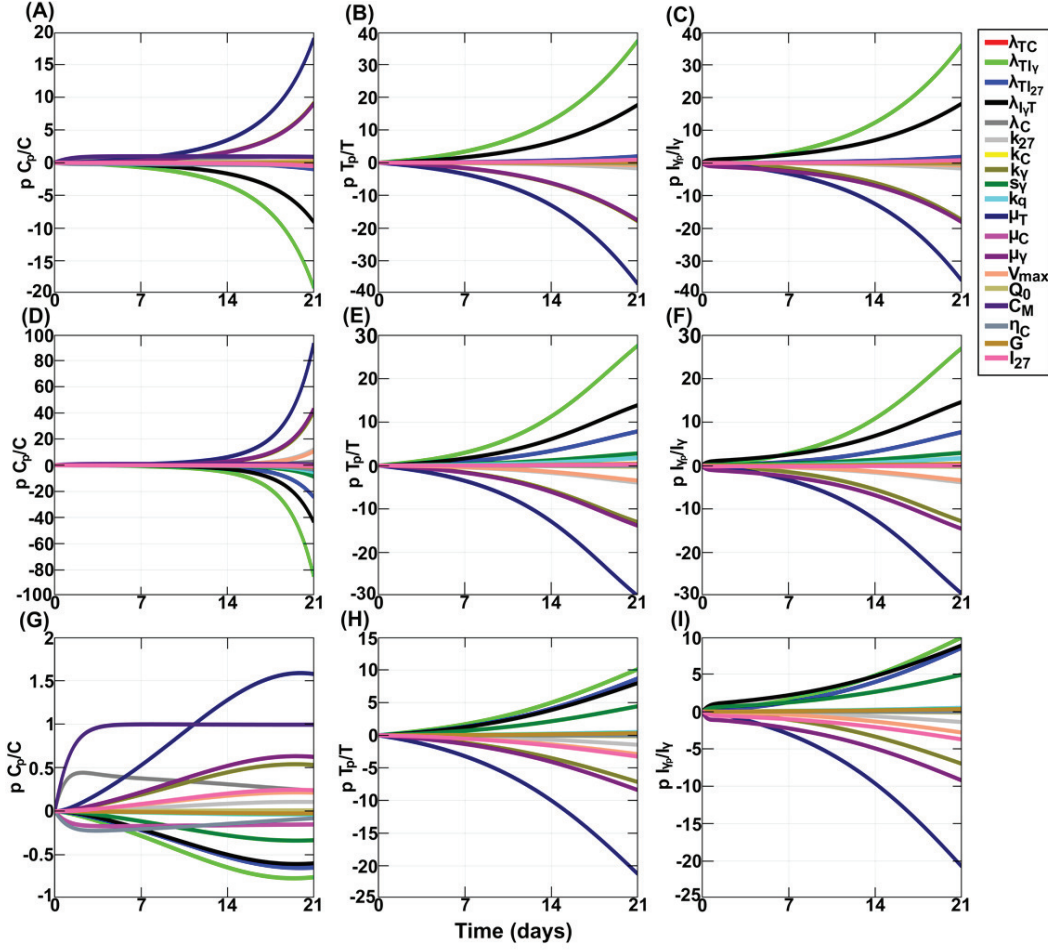
FIGURE 5. **The logarithmic-relative sensitivity curves of model** (4.1) **for group (I).** The first, second, and third rows show the logarithmic-relative sensitivity curves for the model (4.1) with $G = 0.1$ and $I_{27} = 0.1f_0 = 1.1 \times 10^{-7}$ g/cm^3 (case (I-i)), $I_{27} = f_0 = 1.1 \times 10^{-6}$ g/cm^3 (case (I-ii)), and $I_{27} = 5f_0 = 5.5 \times 10^{-6}$ g/cm^3 (case (I-iii)), respectively, to all parameters p. The first, second, and third columns are the results of $p \times C_p(t)/C(t)$, $p \times T_p(t)/T(t)$, and $p \times I_\gamma(t)/I_\gamma$, respectively. The horizontal and vertical axes represent time during $[0, 21]$ days and the normalized value $p \times X_p/X$ for each parameter p and variable X, respectively.

We choose the parameters I_{27}, G, V_{max}, k_q, Q_0, λ_{TC}, λ_{TI_γ}, $\lambda_{TI_{27}}$, $\lambda_{I_\gamma T}$, λ_C, s_γ, and η_C which play an important role in tumor growth and are estimated. In Fig. 4, the dosage of IL-27 affects the functions of IL-27 in tumor growth, so we consider two ranges of I_{27}: (i) low dose of IL-27: $I_{27} \in [0.1f_0, \ f_0] = [0.11, \ 1.1] \times 10^{-6}$ g/cm^3, and (ii) high dose of IL-27: $I_{27} \in [f_0, \ 5f_0] = [1.1, \ 5.5] \times 10^{-6}$ g/cm^3. For the parameter G, we consider the range covering the low efficacy (i.e., $G = 0.01$) and high efficacy (i.e., $G = 1$). Table 3 lists the baselines with units and ranges of the selected parameters.

For each selected parameter, we use the Latin hypercube sampling (LHS) to generate 20000 samples. Since we are interested in the treatment efficacy of IL-27 and anti-PD-1 comparing to the control case, we calculate the partial rank correlation coefficients (PRCCs) and p-values of the selected parameter
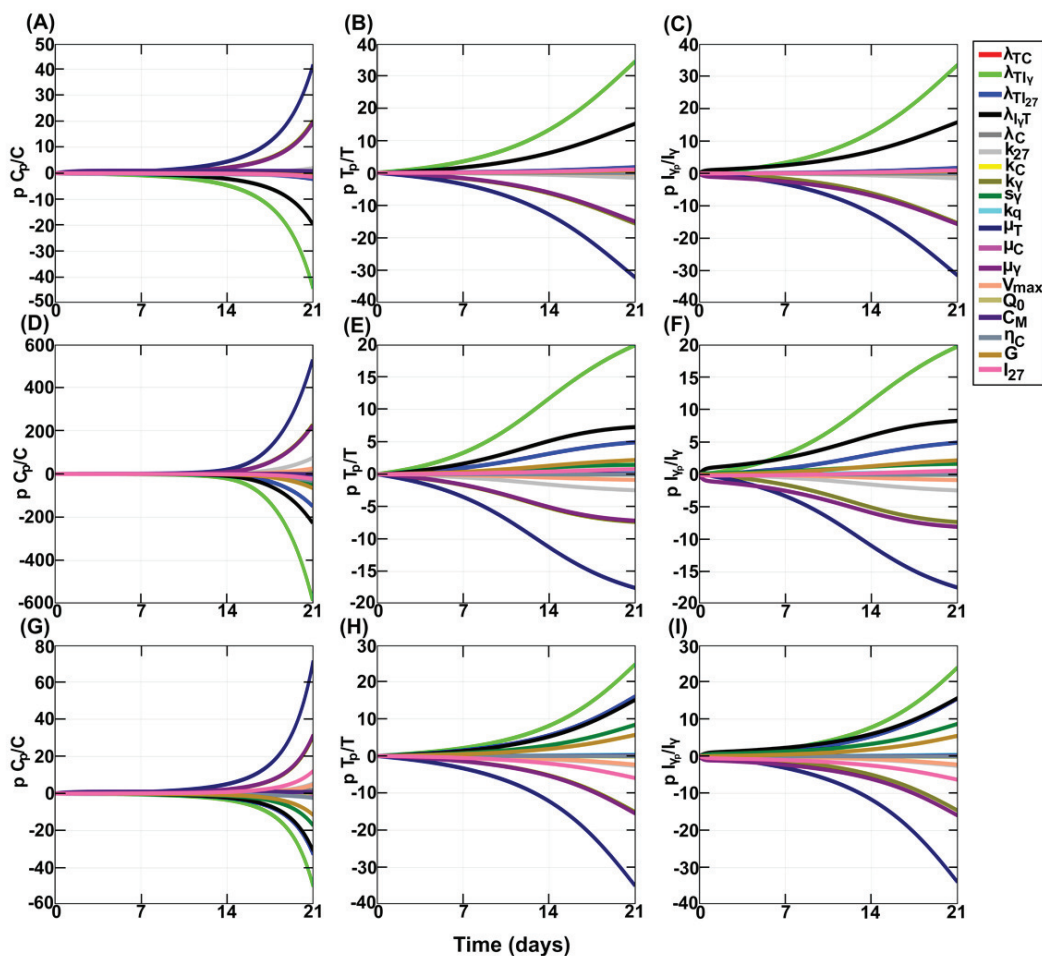
FIGURE 6. **The logarithmic-relative sensitivity curves of model** (4.1) **for group (II).** The first, second, and third rows show the logarithmic-relative sensitivity curves for the model (4.1) with $G = 0.7$ and $I_{27} = 0.1f_0 = 1.1 \times 10^{-7}$ g/cm^3 (case (II-i)), $I_{27} = f_0 = 1.1 \times 10^{-6}$ g/cm^3 (case (II-ii)), and $I_{27} = 5f_0 = 5.5 \times 10^{-6}$ g/cm^3 (case (II-iii)), respectively, to all parameters p. The first, second, and third columns are the results of $p \times C_p(t)/C(t)$, $p \times T_p(t)/T(t)$, and $p \times I_\gamma(t)/I_\gamma$, respectively. The horizontal and vertical axes represent time during $[0, 21]$ days and the normalized value $p \times X_p/X$ for each parameter p and variable X, respectively.

corresponding to the ratio

$$R_2(t) = C^+(t)/C^-(t), \text{ at } t = 21 \text{ } days, \tag{4.1}$$

where $C^+(t)$ and $C^-(t)$ are defined as Eq. (3.1). Thus, for a parameter with positive PRCC (resp. negative PRCC) and p-value smaller than 0.05, increasing this parameter increases (resp. decreases) the ratio R_2 suggesting an improved (resp. reduced) tumor reduction by the dosage of IL-27 and anti-PD-1. The PRCCs of the parameters to C^-, C^+ and R_2 are shown in Table 4.

Table 4 indicates that the dosage of IL-27 does not affect the sign of PRCCs for all parameters, except I_{27} and λ_{TI_γ}. The PRCCs of I_{27} to R_2 and C^+ are negative in the low dose range, whereas they are positive in the high dose range. As shown in Fig. 4, in the low dose range of IL-27, the anti-tumor
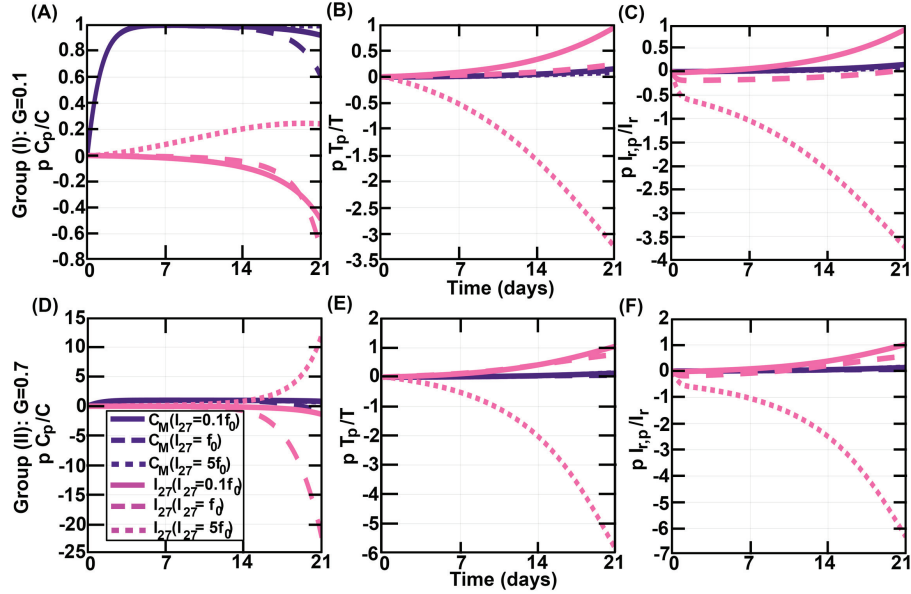
FIGURE 7. **The zoom-in logarithmic-relative sensitivity curves for C_M and I_{27} of model** (4.1). The first and second rows show the zoom-in logarithmic-relative sensitivity curves of C_M and I_{27} for the group (I): $G = 0.1$ and group (II): $G = 0.7$, respectively. The first, second, and third columns are the results of $p \times C_p(t)/C(t)$, $p \times T_p(t)/T(t)$, and $p \times I_\gamma(t)/I_\gamma$, respectively. The horizontal and vertical axes represent time during $[0, 21]$ days and the normalized value $p \times X_p/X$ for the parameter $p \in \{C_M, I_{27}\}$ and variable X, respectively.

reactions of IL-27 are stronger than its pro-tumor reactions, so increasing I_{27} in this regime reduces tumor cell density resulting in the reduction of R_2 and C^+. We obtain opposite outcome of IL-27 when the dose falls in the high dose range. Moreover, regardless of the dose of IL-27, anti-PD-1 always has negative correlation to R_2 and C^+ suggesting that increasing anti-PD-1 always promotes the treatment efficacy. Thus, the results of I_{27} and G agree with the finding in Fig. 4 that IL-27 is anti-tumor in the low dose range and pro-tumor in the high dose range, while anti-PD-1 is always an efficient anti-tumor drug.

The PRCCs of V_{max} to R_2 and C^+ are positive and the PRCCs of k_q to R_2 and C^+ are negative. A higher value of V_{max} induces more PD-1-PD-L1 by IL-27 which inhibits T cell density and increases tumor cell density, resulting in increasing R_2 and C^+. On the other hand, increasing k_q reduces PD-1-PD-L1 by IL-27 which increases T cell density and decreases tumor cell density, resulting in decreasing R_2 and C^+. A higher value of Q_0 represents a higher baseline of PD-1-PD-L1 in the absence of IL-27 resulting in the reduction of T cell density and promotion of tumor cell density C^- in the absence of IL-27 and C^+ in the presence of IL-27. Thus, the PRCCs of Q_0 to C^- and C^+ are positive, regardless of the dosage of IL-27. However, the effect of Q_0 on C^- is stronger than the one on C^+, so the PRCC of Q_0 to R_2 is negative. Increasing the value of λ_{TC} or λ_{TI_γ} or $\lambda_{TI_{27}}$ or $\lambda_{I_\gamma T}$ or s_γ increases the T cell density and then reduces the tumor cell density C^+ and R_2. A higher value of η_C reduces more tumor cell density C^+ and R_2. On the other hand, a higher value of λ_C increases the tumor cell density C^+ and R_2.

TABLE 2. **Sign of $p \times X_p(t)/X(t)$.** The first column lists the parameters. The second to tenth columns (resp. eleventh to the last columns) show the sign for the variables C, T, and I_γ in Group (I) (resp. Group (II)) with $I_{27} = 0.1f_0$, f_0, and $5f_0$. The symbol + (resp. −) represents that the curve $p \times X_p(t)/X(t)$ is positive (resp. negative) during $t \in [0,21]$ *days*. The symbol +/− (resp. −/+) represents that the curve $p \times X_p(t)/X(t)$ changes from positive to negative (resp. changes from negative to positive) in the interval $[0,21]$ *days*.

Parameter	$G=0.1$ $I_{27}=0.1f_0$			$I_{27}=f_0$			$I_{27}=5f_0$			$G=0.7$ $I_{27}=0.1f_0$			$I_{27}=f_0$			$I_{27}=5f_0$		
	C	T	I_γ	C	T	I_γ	C	T	I_γ	C	T	I_γ	C	T	I_γ	C	T	I_γ
I_{27}	-	+	-/+	-	+	-/+	-/+	+/-	-	-	+	-/+	-	+	-/+	-/+	+/-	-
G	-	+	+	-	+	+	-	+	+	-	+	+	-	+	+	-	+	+
k_{27}	+	-	-	+	-	-	+	-	-	+	-	-	+	-	-	+	-	-
k_C	+	-	-	+	-	-	+	-	-	+	-	-	+	-	-	+	-	-
k_γ	+	-	-	+	-	-	+	-	-	+	-	-	+	-	-	+	-	-
μ_T	+	-	-	+	-	-	+	-	-	+	-	-	+	-	-	+	-	-
μ_γ	+	-	-	+	-	-	+	-	-	+	-	-	+	-	-	+	-	-
V_{max}	+	-	-	+	-	-	+	-	-	+	-	-	+	-	-	+	-	-
Q_0	+	-	-	+	-	-	+	-	-	+	-	-	+	-	-	+	-	-
λ_{TC}	-	+	+	-	+	+	-	+	+	-	+	+	-	+	+	-	+	+
λ_{TI_γ}	-	+	+	-	+	+	-	+	+	-	+	+	-	+	+	-	+	+
$\lambda_{TI_{27}}$	-	+	+	-	+	+	-	+	+	-	+	+	-	+	+	-	+	+
$\lambda_{I_\gamma T}$	-	+	+	-	+	+	-	+	+	-	+	+	-	+	+	-	+	+
s_γ	-	+	+	-	+	+	-	+	+	-	+	+	-	+	+	-	+	+
k_q	-	+	+	-	+	+	-	+	+	-	+	+	-	+	+	-	+	+
λ_C	+	+	+	+	+	+	+	+	+	+	+	+	+	+	+	+	+	+
C_M	+	+	+	+	+	+	+	+	+	+/-	+	+	+	+	+	+	+	+
η_C	-	-	-	-	-	-	-	-	-	-	-	-	-	-	-	-	-	-
μ_C	-	-	-	-	-	-	-	-	-	-	-	-	-	-	-	-	-	-

TABLE 3. **Parameters chosen for the global sensitivity analysis.**

Parameter	Range	Baseline
I_{27}	Low IL-27: $[0.11, 1.1] \times 10^{-6}$ g/cm^3	6.05×10^{-7} g/cm^3
	High IL-27: $[1.1, 5.5] \times 10^{-6}$ g/cm^3	3.3×10^{-6} g/cm^3
G	$[0.01, 1]$	0.5
V_{max}	$[0.12, 0.48]$	0.24
k_q	$[0.55, 2.2] \times 10^{-6}$ g/cm^3	1.1×10^{-6} g/cm^3
Q_0	$[0.005, 0.02]$	0.01
λ_{TC}	$[3, 12] \times 10^{-3}/day$	$6 \times 10^{-3}/day$
λ_{TI_γ}	$[0.45, 0.75]/day$	$0.6/day$
$\lambda_{TI_{27}}$	$[0.1316, 0.2194]/day$	$0.1755/day$
$\lambda_{I_\gamma T}$	$[1.242, 2.07] \times 10^{-7}/day$	$1.656 \times 10^{-7}/day$
λ_C	$[1.062, 1.77]/day$	$1.416/day$
s_γ	$[2.2, 8.8] \times 10^{-6}$ g/cm^3	4.4×10^{-6} g/cm^3
η_C	$[115.5, 462]$ $cm^3/g/day$	231 $cm^3/g/day$

TABLE 4. **The PRCC of parameters for the global sensitivity analysis of model** (2.5). The first column lists the cases and the second column lists the corresponding case: C^-, C^+ and R_2. The PRCCs for I_{27}, G, V_{max}, k_q, Q_0, and λ_{TC} (resp. λ_{TI_γ}, $\lambda_{TI_{27}}$, $\lambda_{I_\gamma T}$, λ_C, s_γ, and η_C) are listed from the third to eighth columns in the upper table (resp. the lower table). All the PRCCs are with the p-value smaller than 0.05, except the ones marked with *.

	Case	I_{27}	G	V_{max}	k_q	Q_0	λ_{TC}
Deficient	PRCC for C^-	0.001667*	-0.00836*	0.000818*	-0.00473*	0.05569	-0.07523
Low IL27	PRCC for C^+	-0.2568	-0.3306	0.1875	-0.1185	0.01892	-0.04926
Low IL27	PRCC for R_2	-0.1406	-0.2177	0.1259	-0.08714	-0.02341	-0.003524*
High IL27	PRCC for C^+	0.2973	-0.5707	0.363	-0.1211	0.02973	-0.04565
High IL27	PRCC for R_2	0.2039	-0.4165	0.2545	-0.07761	-0.007648*	-0.0124*
	Case	λ_{TI_γ}	$\lambda_{TI_{27}}$	$\lambda_{I_\gamma T}$	λ_C	s_γ	η_C
Deficient	PRCC for C^-	-0.9245	0.008797*	-0.6919	0.4597	-0.002283*	-0.2376
Low IL27	PRCC for C^+	-0.8733	-0.2778	-0.5497	0.1372	-0.1977	-0.1964
Low IL27	PRCC for R_2	-0.1054	-0.1766	-0.03544	0.02237	-0.1262	-0.02347
High IL27	PRCC for C^+	-0.7871	-0.5035	-0.5176	0.1453	-0.5295	-0.2095
High IL27	PRCC for R_2	0.1984	-0.3517	0.006699*	0.02615	-0.3804	-0.03612

5. MATHEMATICAL ANALYSIS

In this section, we analyze the dynamics of the model (2.5), i.e.,

$$\begin{cases} \dfrac{dC}{dt} = \underbrace{\lambda_C C\left(1 - \dfrac{C}{C_M}\right)}_{\text{Growth}} - \underbrace{\eta_C TC}_{\text{Death by T cells}} - \underbrace{\mu_C C}_{\text{Death}} \\[3ex] \dfrac{dT}{dt} = \left(\underbrace{\lambda_{TC} T \dfrac{C}{k_C + C}}_{\text{Immune Response}} + \underbrace{\lambda_{TI_\gamma} T \dfrac{I_\gamma}{I_\gamma + k_\gamma}}_{\text{Production by IFN-}\gamma} + \underbrace{\lambda_{TI_{27}} T \dfrac{I_{27}}{I_{27} + k_{27}}}_{\text{Production by IL-27}} \right) \times \underbrace{\dfrac{1}{1 + Q(I_{27}) \times (1 - G)}}_{\text{Inhibition by PD-1-PD-L1 Complex}} - \underbrace{\mu_T T}_{\text{Death}} \\[3ex] \dfrac{dI_\gamma}{dt} = \underbrace{\lambda_{I_\gamma T} T \dfrac{s_\gamma}{s_\gamma + I_{27}}}_{\text{Production by T cells}} - \underbrace{\mu_\gamma I_\gamma}_{\text{Decay}}. \end{cases}$$

For simplicity, we only consider the cases without anti-PD-1, i.e., $G = 0$. We analyze the invariant set and boundedness, as well as the existence, uniqueness, and stability of the equilibrium. We also provide numerical examples to investigate the uniqueness and stability of equilibria, under certain parameter setting.

5.1. **Mathematical Analysis of Basic Dynamics.** Denote the solution of the model (2.5) to be $X(t) = (C(t), T(t), I_\gamma(t))$ with initial condition $X(0) = (C(0), T(0), I_\gamma(0))$. We first show that the $R_+^3 := \{(x_1, x_2, x_3) \in R^3 | x_i \geq 0, \ i = 1, 2, 3\}$ is an invariant set of model (2.5) and any solution $X(t)$ of the model (2.5) is bounded under some condition.

Proposition 5.1. $X(t) \in R_+^3 := \{(x_1, x_2, x_3) \in R^3 | x_i \geq 0, \ i = 1, 2, 3\}$ *provided* $X(0) \in R_+^3$.

Proof. First, we consider $C(0) > 0$, $T(0) > 0$, $I_\gamma(0) > 0$. By using contradiction, we assume that the component $C(t)$ is the first component reaches zero, namely, there exists $t_1 > 0$ such that $C(t_1) = 0$,

$T(t_1) > 0$, $I_\gamma(t_1) > 0$, and $C(t) > 0$ if $0 \le t < t_1$. Then we have

$$\frac{dC}{dt}(t_1) = \lambda_C C(t_1)\left(1 - \frac{C(t_1)}{C_M}\right) - \eta_C T(t_1)C(t_1) - \mu_C C(t_1) = 0, \text{ with } C(t_1) = 0, \qquad (5.1)$$

which implies $C(t) \equiv 0$ for all $t \ge 0$. This result contradicts to $C(0) > 0$, so $C(t) > 0$ for all t. Using the same argument, we have $T(t) \ge 0$ and $I_\gamma(t) \ge 0$ for all t, if $T(0) > 0$ and $I_\gamma(0) > 0$. By using a similar argument, if $C(0) = 0$ or $T(0) = 0$ or $I_\gamma(0) = 0$, then we have $C(t) \equiv 0$ or $T(t) \equiv 0$ or $I_\gamma \equiv 0$, for all $t \ge 0$. $\qquad\square$

Proposition 5.2. *If $X(0) \in R_+^3$ and $\lambda_{TC} + \lambda_{TI_\gamma} + \lambda_{TI_{27}} < \mu_T$, then the solution $X(t)$ of the model* (2.5) *is bounded.*

Proof. Since $X(0) \in R_+^3$, all solutions are nonnegative. For Eq. (2.1), we have

$$C'(t) = \lambda_C C\left(1 - \frac{C}{C_M}\right) - \eta_C TC - \mu_C C \le \lambda_C C\left(1 - \frac{C}{C_M}\right) =: F_1(C).$$

Since the solution of $z' = F_1(z)$ converges to C_M, $C(t)$ is bounded by the differential inequality. Similarly, for Eq. (2.2), we obtain

$$\begin{aligned} T' &= \left(\lambda_{TC}T\frac{C}{k_C + C} + \lambda_{TI_\gamma}T\frac{I_\gamma}{I_\gamma + k_\gamma} + \lambda_{TI_{27}}T\frac{I_{27}}{I_{27} + k_{27}}\right) \times \frac{1}{1 + Q(I_{27})} - \mu_T T \\ &\le (\lambda_{TC} + \lambda_{TI_\gamma} + \lambda_{TI_{27}} - \mu_T)T =: F_2(T). \end{aligned}$$

Thus, $T(t)$ is bounded and converges to zero, because the solution of $z' = F_2(z)$ converges to zero when $\lambda_{TC} + \lambda_{TI_\gamma} + \lambda_{TI_{27}} < \mu_T$. For Eq. (2.4), we have

$$I_\gamma' = \lambda_{I_\gamma}T T\frac{s_\gamma}{I_{27} + s_\gamma} - \mu_\gamma I_\gamma \le \lambda_{I_\gamma}T T - \mu_\gamma I_\gamma \to \mu_\gamma I_\gamma \text{ as } t \to \infty,$$

and hence I_γ is bounded. $\qquad\square$

Propositions 5.1 and 5.2 show that the solutions of model (2.5) are bounded and positive under some conditions, which provide the existence of solution. In the following, we analyze the existence, uniqueness, and stability of the equilibria of the model (2.5) to investigate the local dynamics of the model (2.5).

We define a polynomial $P(T)$ as

$$P(T) := \beta_2 T^2 + \beta_1 T + \beta_0, \qquad (5.2)$$

with

$$\beta_2 = -R\lambda_{I_\gamma T}S_\gamma C_M \eta_C + \tilde{Q}\lambda_{TC}C_M\lambda_{I_\gamma T}\eta_C S_\gamma + \tilde{Q}\lambda_{TI_\gamma}\lambda_{I_\gamma T}S_\gamma C_M \eta_C,$$

$$\begin{aligned} \beta_1 &= -RC_M\eta_C k_\gamma \mu_\gamma + \tilde{Q}C_M\eta_C k_\gamma \lambda_{TC}\mu_\gamma + RC_M\lambda_C\lambda_{I_\gamma T}S_\gamma + Rk_C\lambda_C\lambda_{I_\gamma T}S_\gamma, \\ &\quad - \tilde{Q}\lambda_C\lambda_{I_\gamma T}S_\gamma(C_M\lambda_{TC} + C_M\lambda_{TI_\gamma} + k_C\lambda_{TI_\gamma}) + \tilde{Q}C_M\lambda_{I_\gamma T}\mu_C S_\gamma(\lambda_{TC} + \lambda_{TI_\gamma}) \\ &\quad - RC_M\lambda_{I_\gamma T}\mu_C S_\gamma, \end{aligned}$$

$$\beta_0 = Rk_\gamma C_M\lambda_C\mu_\gamma + Rk_\gamma k_C\lambda_C\mu_\gamma - Rk_\gamma C_M\mu_C\mu_\gamma - k_\gamma\tilde{Q}\lambda_{TC}C_M\lambda_C\mu_\gamma + \tilde{Q}\lambda_{TC}\mu_C C_M k_\gamma\mu_\gamma, \qquad (5.3)$$

$$R = \mu_T - \tilde{Q}\lambda_{TI_{27}}\frac{I_{27}}{k_{27} + I_{27}},$$

$$\tilde{Q} = \frac{1}{1 + Q(I_{27})},$$

$$S_\gamma = \frac{s_\gamma}{s_\gamma + I_{27}}.$$

Proposition 5.3. *The model* (2.5) *always has three equilibria:*

$$E_0 = (C_0, T_0, I_{\gamma,0}) = (0,0,0), \; E_1 = (C_1, T_1, I_{\gamma,1}) = (C_M(1 - \mu_C/\lambda_C), 0, 0), \; and \; .$$
$$E_2 = (C_2, T_2, I_{\gamma,2}) = (0, T_2, I_{\gamma,2}),$$

with

$$I_{\gamma,2} = \frac{\lambda_{I_\gamma T} s_\gamma}{(s_\gamma + I_{27})\mu_\gamma} T_2 \; and \; T_2 = \frac{\mu_\gamma k_\gamma (s_\gamma + I_{27})(\mu_T(I_{27} + k_{27}) - \lambda_{TI_{27}} I_{27} \tilde{Q})}{\lambda_{I_\gamma T} s_\gamma (\lambda_{TI_\gamma} \tilde{Q}(I_{27} + k_{27}) + \lambda_{TI_{27}} \tilde{Q} I_{27} - \mu_T(I_{27} + k_{27}))}.$$

Moreover,

(i) *if* $\lambda_C > \mu_C$, *then* E_1 *is a non-negative equilibrium of the model* (2.5); *and*

(ii) *if* $0 < \mu_T - \lambda_{TI_{27}} \tilde{Q} I_{27}/(I_{27} + k_{27}) < \lambda_{TI_\gamma} \tilde{Q}$, *then* E_2 *is a non-negative equilibrium of the model* (2.5), *with* $\tilde{Q}$ *defined as Eq.* (5.3).

Proof. An equilibrium $E_* = (C^*, T^*, I_\gamma^*)$ of model (2.5) satisfies:

$$\lambda_C C^* \left(1 - \frac{C^*}{C_M}\right) - \eta_C T^* C^* - \mu_C C^* = 0, \tag{5.4}$$

$$\left(\lambda_{TC} T^* \frac{C^*}{C^* + k_C} + \lambda_{TI_\gamma} T^* \frac{I_\gamma^*}{I_\gamma^* + k_\gamma} + \lambda_{TI_{27}} T^* \frac{I_{27}}{I_{27} + k_{27}}\right) \frac{1}{1 + Q(I_{27})} - \mu_T T^* = 0, \tag{5.5}$$

$$\lambda_{I_\gamma T} T^* \frac{s_\gamma}{s_\gamma + I_{27}} - \mu_\gamma I_\gamma^* = 0. \tag{5.6}$$

Eqs. (5.4) and (5.6) imply

$$I_\gamma^* = \frac{\lambda_{I_\gamma T} s_\gamma}{(s_\gamma + I_{27})\mu_\gamma} T^* \tag{5.7}$$

and

$$C^* = 0 \; or \; C^* = \frac{C_M}{\lambda_C}(\lambda_C - \eta_C T^* - \mu_C). \tag{5.8}$$

Hence, when $T^* = 0$, we have the trivial equilibrium $E_0 = (0,0,0)$ and the equilibrium $E_1 = (C_M - C_M \mu_C/\lambda_C, 0, 0)$. Notice that E_1 is a non-negative equilibrium if $\lambda_C > \mu_C$.

We obtain E_2 by setting $C^* = 0$ and $T^* \neq 0$, so we have

$$\lambda_{TI_\gamma} \tilde{Q} \frac{I_\gamma^*}{I_\gamma^* + k_\gamma} + \lambda_{TI_{27}} \tilde{Q} \frac{I_{27}}{I_{27} + k_{27}} - \mu_T = 0. \tag{5.9}$$

Substitute Eq. (5.7) into Eq. (5.9), we have

$$T_2 = T^* = \frac{\mu_\gamma k_\gamma (s_\gamma + I_{27})(\mu_T(I_{27} + k_{27}) - \lambda_{TI_{27}} I_{27} \tilde{Q})}{\lambda_{I_\gamma T} s_\gamma (\lambda_{TI_\gamma} \tilde{Q}(I_{27} + k_{27}) + \lambda_{TI_{27}} \tilde{Q} I_{27} - \mu_T(I_{27} + k_{27}))},$$
$$I_{\gamma,2} = I_\gamma^* = \frac{\lambda_{I_\gamma T} s_\gamma}{(s_\gamma + I_{27})\mu_\gamma} T_2 \tag{5.10}$$

and hence $E_2 = (0, T_2, I_{\gamma,2})$. If $0 < \mu_T - \lambda_{TI_{27}} \tilde{Q} I_{27}/(I_{27} + k_{27}) < \lambda_{TI_\gamma} \tilde{Q}$, then $\lambda_{TI_\gamma} \tilde{Q}(I_{27} + k_{27}) + \lambda_{TI_{27}} \tilde{Q} I_{27} - \mu_T(I_{27} + k_{27}) > 0$ and $T_2 > 0$. □

Proposition 5.4. *For the* β_i *defined as Eq.* (5.3), *if either*

$$(i) \; \beta_2 > 0, \; \beta_1 < 0, \; \beta_1^2 - 4\beta_2\beta_0 \geq 0, \tag{5.11}$$

or

$$(ii) \; \beta_2 < 0, \; \beta_1 > 0, \; \beta_1^2 - 4\beta_2\beta_0 \leq 0 \tag{5.12}$$

holds, then the polynomial $P(T)$ defined as Eq. (5.2) has at least one positive real root T^*. Furthermore, if $0 < T^* < \frac{\lambda_C - \mu_C}{\eta_C}$, then the model (2.5) has at least one positive equilibrium E^+ or E^- defined as

$$E_+ = (C^+, T^+, I_\gamma^+) \text{ and } E_- = (C^-, T^-, I_\gamma^-)$$

where

$$C^+ = \frac{C_M}{\lambda_C}(\lambda_C - \eta_C T^+ - \mu_C), \ T^+ = \frac{-\beta_1 + \sqrt{\beta_1^2 - 4\beta_2\beta_0}}{2\beta_2}, \ I_\gamma^+ = \lambda_{I_\gamma T} T^+ \frac{s_\gamma}{\mu_\gamma(s_\gamma + I_{27})}, \ (5.13)$$

$$C^- = \frac{C_M}{\lambda_C}(\lambda_C - \eta_C T^- - \mu_C), \ T^- = \frac{-\beta_1 - \sqrt{\beta_1^2 - 4\beta_2\beta_0}}{2\beta_2}, \ I_\gamma^- = \lambda_{I_\gamma T} T^- \frac{s_\gamma}{\mu_\gamma(s_\gamma + I_{27})}. \ (5.14)$$

Proof. We first consider the condition (i), i.e., $\beta_2 > 0$, $\beta_1 < 0$ and $\beta_1^2 - 4\beta_2\beta_0 \geq 0$, then $\frac{d^2P}{dT^2} = 2\beta_2 > 0$ implies that $P(T)$ is concave up and we can rewrite $P(T)$ as

$$P(T) = \beta_2 \left(T + \frac{\beta_1}{2\beta_2} \right)^2 + \beta_0 - \frac{\beta_1^2}{4\beta_2}. \tag{5.15}$$

Moreover, the condition (5.11) implies $-\frac{\beta_1}{2\beta_2} > 0$ and $\beta_0 - \frac{\beta_1^2}{4\beta_2} \leq 0$. Thus, $P(T)$ has at least one positive real root T^*.

Next, we consider the condition (ii), i.e. $\beta_2 < 0$, $\beta_1 > 0$ and $\beta_1^2 - 4\beta_2\beta_0 \leq 0$, then $\frac{d^2P}{dT^2} = 2\beta_2 < 0$ implies that $P(T)$ is concave down. Moreover, the condition (5.11) implies $-\frac{\beta_1}{2\beta_2} > 0$ and $\beta_0 - \frac{\beta_1^2}{4\beta_2} \geq 0$. Thus, $P(T)$ has at least one positive real root T^*. For the equilibrium E_+, as defined in Eq. (5.13), we obtain T^+ by solving the positive root of $P(T)$, i.e., $T^+ = \frac{-\beta_1 + \sqrt{\beta_1^2 - 4\beta_2\beta_0}}{2\beta_2}$. If $0 < T^+ < \frac{\lambda_C - \mu_C}{\eta_C}$, then T^+, I_γ^+, and C^+ are positive and hence E_+ is a positive equilibrium. A similar argument holds for E_-. $\square$

Next, we provide the stability analysis of each equilibrium mentioned in Propositions 5.3 and 5.4.

Proposition 5.5. *(i) The trivial equilibrium $E_0 = (C_0, T_0, I_{\gamma,0}) = (0,0,0)$ is locally asymptotically stable, if*

$$\lambda_C < \mu_C \quad and \quad \tilde{Q}\lambda_{TI_{27}} \frac{I_{27}}{I_{27} + k_{27}} < \mu_T. \tag{5.16}$$

(ii) The equilibrium $E_1 = (C_1, T_1, I_{\gamma,1}) = (C_M - C_M\mu_C/\lambda_C, 0, 0)$ is locally asymptotically stable, if

$$\lambda_C > \mu_C \quad and \quad \frac{\tilde{Q}\lambda_{TC}C_1}{C_1 + k_C} + \tilde{Q}\lambda_{TI_{27}} \frac{I_{27}}{I_{27} + k_{27}} < \mu_T. \tag{5.17}$$

(iii) The equilibrium $E_2 = (C_2, T_2, I_{\gamma,2}) = (0, T_2, I_{\gamma,2})$ is unstable, if

$$\lambda_C - \mu_C - \eta_C T_2 \neq 0. \tag{5.18}$$

(iv) The equilibrium $E_* = (C_*, T_*, I_{\gamma,*})$, with $* \in \{+, -\}$, is locally asymptotically stable, if and only if $S_1 > 0$, $S_2 S_1 - S_3 > 0$, and $S_3 > 0$ where

$$\begin{aligned} S_1 &= -J_{11} - J_{22} - J_{33}, \\ S_2 &= J_{11}J_{22} + J_{11}J_{33} + J_{22}J_{33} - J_{32}J_{23} - J_{21}J_{12}, \\ S_3 &= J_{11}J_{32}J_{23} + J_{33}J_{12}J_{22} - J_{33}J_{11}J_{22}. \end{aligned} \tag{5.19}$$

and

$$J_{11} = \lambda_C - \mu_C - \frac{2\lambda_C}{C_M}C_* - \eta_C T_*, \ J_{12} = -\eta_C C_*,$$

$$J_{21} = \frac{\tilde{Q}\lambda_{TC}k_C T_*}{(C_* + k_C)^2}, \ J_{22} = \lambda_{TC}\tilde{Q}\frac{C_*}{k_C + C_*} + \lambda_{TI_\gamma}\tilde{Q}\frac{I_\gamma^n}{k_\gamma + I_{\gamma,*}} + \lambda_{TI_{27}}\tilde{Q}\frac{I_{27}}{k_{27} + I_{27}} - \mu_T, \ (5.20)$$

$$J_{23} = \frac{\tilde{Q}\lambda_{TI_\gamma}k_\gamma T_*}{(I_{\gamma,*} + k_\gamma)^2}, \ J_{32} = \lambda_{I_\gamma T}\frac{s_\gamma}{s_\gamma + I_{27}}, \ J_{33} = -\mu_\gamma,$$

Proof. The Jacobian matrix J_* at the equilibrium $E_* = (C^*, T^*, I_\gamma^*)$ with $* \in \{0, 1, 2, +, -\}$ of the model (2.5) is

$$\begin{bmatrix} \lambda_C - \mu_C - \frac{2\lambda_C}{C_M}C^* - \eta_C T^* & -\eta_C C^* & 0 \\ \frac{\tilde{Q}\lambda_{TC}k_C T^*}{(C^*+k_C)^2} & \lambda_{TC}\tilde{Q}\frac{C^*}{k_C+C^*} + \lambda_{TI_\gamma}\tilde{Q}\frac{I_\gamma^*}{k_\gamma+I_\gamma^*} + \lambda_{TI_{27}}\tilde{Q}\frac{I_{27}}{k_{27}+I_{27}} - \mu_T & \frac{\tilde{Q}\lambda_{TI_\gamma}k_\gamma T^*}{(I_\gamma^*+k_\gamma)^2} \\ 0 & \lambda_{I_\gamma T}\frac{s_\gamma}{s_\gamma+I_{27}} & -\mu_\gamma \end{bmatrix}$$

$$(5.21)$$

where $\tilde{Q}$ is defined as Eq. (5.2).

For the equilibrium $E_0 = (C_0, T_0, I_{\gamma,0}) = (0, 0, 0)$, we have the Jacobian matrix J_0 as follows

$$J_0 = \begin{bmatrix} \lambda_C - \mu_C & 0 & 0 \\ 0 & \lambda_{TI_{27}}\tilde{Q}\frac{I_{27}}{k_{27}+I_{27}} - \mu_T & 0 \\ 0 & \lambda_{I_\gamma T}\frac{s_\gamma}{s_\gamma+I_{27}} & -\mu_\gamma \end{bmatrix} \qquad (5.22)$$

with eigenvalues $\lambda_C - \mu_C$, $-\mu_\gamma$, and $\tilde{Q}\lambda_{TI_{27}}I_{27}/(I_{27} + k_{27}) - \mu_T$. Thus, the condition (5.16) implies all eigenvalues are negative and hence E_0 is locally asymptotically stable.

For the equilibrium $E_1 = (C_1, T_1, I_{\gamma,1}) = (C_M - C_M\mu_C/\lambda_C, 0, 0)$, it is a non-negative equilibrium if $\lambda_C > \mu_C$, due to Proposition 5.3. By using Eq. (5.21), we have the Jacobian matrix J_1 as

$$J_1 = \begin{bmatrix} \mu_C - \lambda_C & -\eta_C C_1 & 0 \\ 0 & \lambda_{TC}\tilde{Q}\frac{C_1}{k_C+C_1} + \lambda_{TI_{27}}\tilde{Q}\frac{I_{27}}{k_{27}+I_{27}} - \mu_T & 0 \\ 0 & \lambda_{I_\gamma T}\frac{s_\gamma}{s_\gamma+I_{27}} & -\mu_\gamma \end{bmatrix} \qquad (5.23)$$

with $C_1 = C_M - C_M\mu_C/\lambda_C$ having the eigenvalues

$$-\mu_\gamma, \ \mu_C - \lambda_C, \ \frac{\tilde{Q}\lambda_{TC}C_1}{C_1 + k_C} + \tilde{Q}\lambda_{TI_{27}}\frac{I_{27}}{I_{27} + k_{27}} - \mu_T.$$

Thus, the condition (5.17) implies all eigenvalues are negative and hence E_1 is locally asymptotically stable.

Next, for the equilibrium $E_2 = (C_2, T_2, I_{\gamma,2}) = (0, T_2, I_{\gamma,2})$, we obtain the Jacobian matrix J_2 as

$$J_2 = \begin{bmatrix} \lambda_C - \mu_C - \eta_C T_2 & 0 & 0 \\ \frac{\tilde{Q}\lambda_{TC}T_2}{k_C} & 0 & \frac{\tilde{Q}\lambda_{TI_\gamma}k_\gamma T_2}{(I_{\gamma,2}+k_\gamma)^2} \\ 0 & \lambda_{I_\gamma T}\frac{s_\gamma}{s_\gamma+I_{27}} & -\mu_\gamma \end{bmatrix} \qquad (5.24)$$

The characteristic equation of J_2 is in the form $(\lambda_C - \mu_C - \eta_C T_2 - \lambda)(\lambda^2 + a\lambda - b)$, with $a > 0$ and $b > 0$. The factor $(\lambda_C - \mu_C - \eta_C T_2 - \lambda)$ provides one eigenvalue $\lambda_C - \mu_C - \eta_C T_2$. The other factor $(\lambda^2 + a\lambda - b)$ has one positive real root and one negative real root, due to $a > 0$ and $b > 0$. Hence, the condition (5.18) implies E_2 is always unstable.

Finally, about the equilibrium $E_* = (C_*, T_*, I_{\gamma,*})$ with $* \in \{+, -\}$, the corresponding Jacobian matrix J_* is

$$J_* = \begin{bmatrix} J_{11} & J_{12} & 0 \\ J_{21} & J_{22} & J_{23} \\ 0 & J_{32} & J_{33} \end{bmatrix} \tag{5.25}$$

where J_{ij} are defined as Eq. (5.20). The characteristic equation of J_* is

$$P_{J_*}(\lambda) = \lambda^3 + S_1\lambda^2 + S_2\lambda + S_3, \tag{5.26}$$

where S_i are defined as Eq. (5.19). Hence, by applying the Routh-Hurwitz criterion, E_* is locally asymptotically stable, if and only if $S_1 > 0$, $S_2S_1 - S_3 > 0$, and $S_3 > 0$. □

5.2. **Numerical Example.** In this subsection, we provide one example to investigate how the parameter values affect the existence and stability of all equilibria E_0, E_1, E_2, E_+, and E_-, in the absence of anti-PD-1 (i.e., $G = 0$).

Based on the Proposition 5.5, we vary the parameter values I_{27}, λ_{TC}, and $\lambda_{TI_{27}}$ from certain ranges and then choose the values of other parameters from Table 5. For each set of $(I_{27}, \lambda_{TC}, \lambda_{TI_{27}})$, E_0, E_1, and E_2 always exist due to Proposition 5.3, but the existence of E_+ and E_- depends on the conditions mentioned in Proposition 5.4. Thus, for any fixed $(I_{27}, \lambda_{TC}, \lambda_{TI_{27}})$, we first verify the existence of E_+ and E_- and then analyze their stability by calculating the eigenvalues of the corresponding Jacobian matrix defined as Eq. (5.21). Next, we define the function $F_*(I_{27}, \lambda_{TC}, \lambda_{TI_{27}})$ as

$$F_*(I_{27}, \lambda_{TC}, \lambda_{TI_{27}}) = \begin{cases} 1 & \text{, if } E_* \text{ is locally asymptotically stable} \\ -1 & \text{, if } E_* \text{ is unstable} \\ 0 & \text{, if } E_* \text{ does not exist} \end{cases},$$

to represents the stability of E_* at the fixed parameter values $(I_{27}, \lambda_{TC}, \lambda_{TI_{27}})$, with $* \in \{0, 1, 2, +, -\}$.

Fig. 8 shows the value of $F_*(I_{27}, \lambda_{TC}, \lambda_{TI_{27}})$ for the equilibrium E_* with $* \in \{0, 1, 2, +, -\}$, where $\lambda_{TC} \in [0, 0.6]/day$ and $\lambda_{TI_{27}} \in [0, 1]/day$, and

$$I_{27} \in \{0,\ 0.5f_0,\ f_0,\ 1.5f_0,\ 2f_0\}, \text{ with } f_0 = 1.1 \times 10^{-6} \ g/cm^3.$$

In Fig. 8, we find that the trivial equilibrium E_0 is unstable and the positive equilibrium E_+ does not exist, for any selected $(I_{27}, \lambda_{TC}, \lambda_{TI_{27}})$. The result of E_0 suggests that the tumor cells, T cells, and IFN-γ will not all vanish.

In the absence of IL-27 (i.e., $I_{27} = 0$), the non-negative equilibrium $E_1 = (C_M(1 - \frac{\mu_C}{\lambda_C}), 0, 0)$ is unstable if $\lambda_{TC} > 0.4932/day$, and is locally asymptotically stable if $\lambda_{TC} < 0.4932/day$, for any $\lambda_{TI_{27}} \in [0, 1]/day$. Note that the $\lambda_{TI_{27}}$ vanishes when $I_{27} = 0$, so $\lambda_{TI_{27}}$ does not affect the result of any equilibrium in the absence of IL-27. The above result indicates that tumor cells cannot be eliminated when the immune response is weak (namely, λ_{TC} is relatively small), in the absence of IL-27. However, in the presence of IL-27, the stability of E_1 switches from locally asymptotically stable to unstable, as $\lambda_{TI_{27}}$ increases. Moreover, as I_{27} increases, this stability switching appears at a smaller value of $\lambda_{TI_{27}}$. On the other hand, the positive equilibrium E_- has a similar pattern to E_1 but with different stability. The equilibrium E_- exists and is unstable when E_1 is locally asymptotically stable, for any selected $(I_{27}, \lambda_{TC}, \lambda_{TI_{27}})$.

Additionally, for the equilibrium E_1, we mark the border between the unstable and locally asymptotically stable regions to be a critical curve $\Gamma(\lambda_{TI_{27}})$ which depends on the value of $\lambda_{TI_{27}}$. In the absence of IL-27, the curve $\Gamma(\lambda_{TI_{27}})$ is a horizontal line and is independent of $\lambda_{TI_{27}}$, i.e., $\Gamma(\lambda_{TI_{27}}) = 0.4932$, for any $\lambda_{TI_{27}} \in [0, 1]/day$. In the presence of IL-27, the curve $\Gamma(\lambda_{TI_{27}})$ is linearly decreasing, as $\lambda_{TI_{27}}$

TABLE 5. **Parameter Values for Numerical Example**

Parameter	Value
λ_{TC}	$[0, 0.6]/day$
λ_{TI_γ}	$0.6/day$
$\lambda_{TI_{27}}$	$[0, 1]/day$
$\lambda_{I_\gamma T}$	$1.656 \times 10^{-7}/day$
λ_C	$1.416/day$
k_{27}	$1.1 \times 10^{-6}\ g/cm^3$
k_C	$0.4965\ g/cm^3$
k_γ	$4.5 \times 10^{-11}\ g/cm^3$
s_γ	$4.4 \times 10^{-6}\ g/cm^3$
k_q	$1.1 \times 10^{-6}\ g/cm^3$
μ_T	$0.3/day$
μ_C	$0.173/day$
μ_γ	$3.68/day$
V_{max}	0.24
Q_0	0.01
C_M	$0.9\ g/cm^3$
η_C	$231\ cm^3/g/day$
I_{27}	$[0, 2.2] \times 10^{-6}\ g/cm^3$
G	0

is increasing. Similarly, the critical curve $\Gamma(\lambda_{TI_{27}})$ also appears in the stability pattern of E_- that it is the border between the unstable region (i.e., the blue region) and absence region (i.e., the green region) of E_-. Combining the stability of E_1 and E_- suggests that the model (2.5) has a saddle-note bifurcation at the critical curve $\Gamma(\lambda_{TI_{27}})$, for the bifurcation parameter λ_{TC} in the absence of IL-27 and for the bifurcation parameter $\lambda_{TI_{27}}$ in the presence of IL-27. Thus, when there is no IL-27, the solution approaches the tumor persistence equilibrium E_1 as λ_{TC} decreases indicating that the tumor persistence appears when the immune response is weak (namely, a lower value of λ_{TC}). However, in the presence of IL-27, the solution approaches the tumor persistence equilibrium E_1 as λ_{TC} or $\lambda_{TI_{27}}$ decreases suggesting that the tumor persistence appears when the production rate of T cells by IL-27 is low or the concentration of IL-27 is low.

Finally, we consider the non-negative equilibrium $E_2 = (0, T_2, I_{\gamma,2})$. In the absence of IL-27, the E_2 is unstable for any given λ_{TC} and $\lambda_{TI_{27}}$. However, in the presence of IL-27, there exists a decreasing critical function $\theta(I_{27})$ depending on I_{27} such that the E_2 exists and is unstable when $\lambda_{TI_{27}} < \theta(I_{27})$. This result indicates that the tumor cells cannot be eliminated when the production rate of T cells by IL-27 is low (namely, a lower value of $\lambda_{TI_{27}}$).

In summary, the model (2.5) has at most four equilibria under the parameter setting shown in Table 5. The trivial equilibrium $E_0 = (0, 0, 0)$ and the non-negative equilibrium $E_2 = (0, T_2, I_{\gamma,2})$ represent the tumor elimination case, while the non-negative equilibrium $E_1 = (C_M(1 - \frac{\mu_C}{\lambda_C}), 0, 0)$ and the positive equilibrium $E_- = (C_-, T_-, I_{\gamma,-})$ account for the tumor persistence case. Only the equilibrium E_1 can be locally asymptotically stable when I_{27} or $\lambda_{TI_{27}}$ is small. Other equilibria either is unstable or do not exist. Therefore, when the production rate of T cells by IL-27 is low or the concentration of IL-27 is low, the T cells and IFN-γ could vanish and tumor cells preserve.
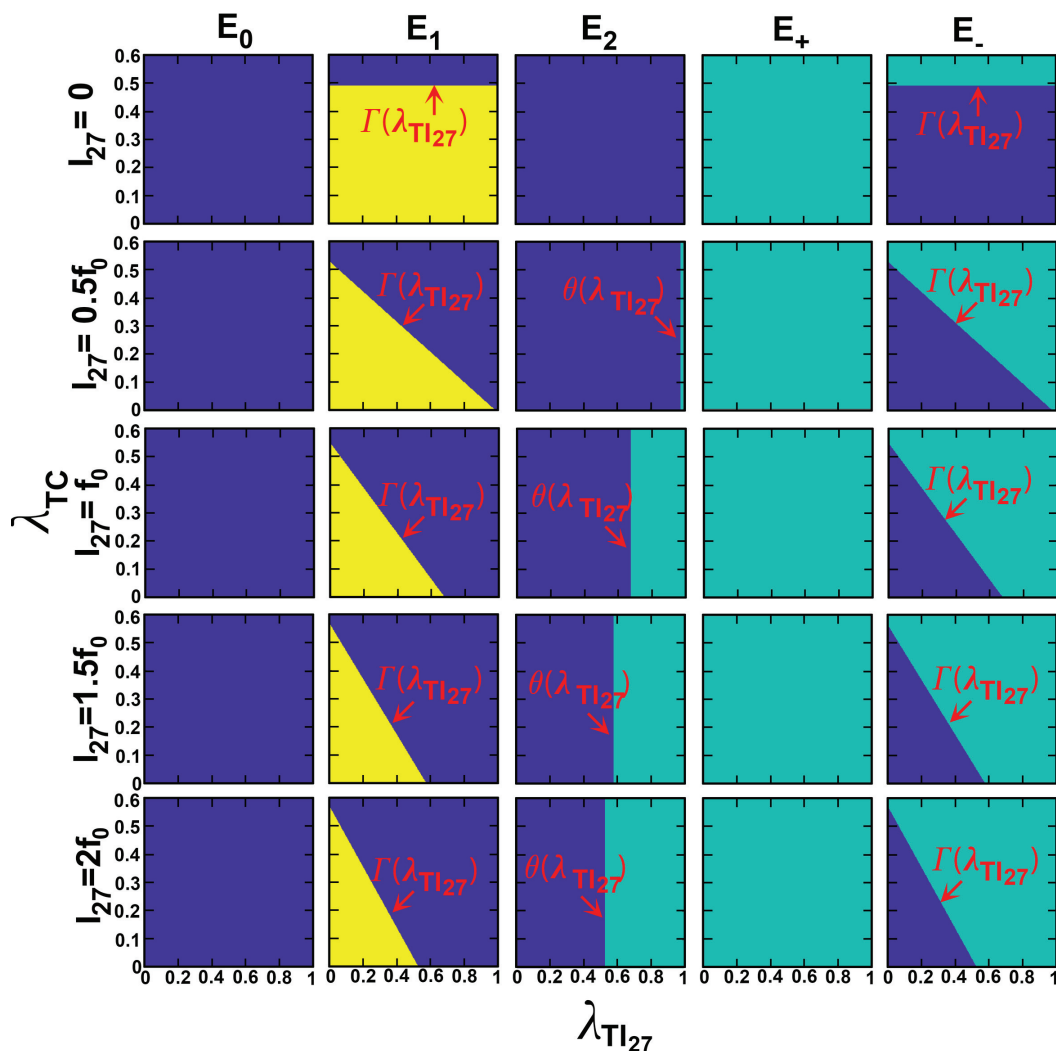
FIGURE 8. **Stability of all equilibria under different values of** I_{27}**.** The first, second, third, fourth, and fifth columns show the stability function $F_*(I_{27}, \lambda_{TC}, \lambda_{TI_{27}})$ for the equilibria E_0, E_1, E_2, E_+, and E_-, respectively. The first, second, third, fourth, and fifth rows display the stability function for all equilibria, when $I_{27} = 0$, $0.5f_0$, f_0, $1.5f_0$, and $2f_0$, respectively. For each plot, the horizontal and vertical axis represent the values of $\lambda_{TI_{27}} \in [0,1]/day$ and $\lambda_{TC} \in [0,0.6]/day$, respectively, which are equally divided into 251 grids. The green region indicates that the corresponding equilibrium does not exist, i.e., $F_*(I_{27}, \lambda_{TC}, \lambda_{TI_{27}}) = 0$. The yellow region (resp. the blue region) accounts for $F_*(I_{27}, \lambda_{TC}, \lambda_{TI_{27}}) = 1$ (resp. $F_*(I_{27}, \lambda_{TC}, \lambda_{TI_{27}}) = -1$) which means that the corresponding equilibrium is locally asymptotically stable (resp. unstable). The critical curves $\Gamma(\lambda_{TI_{27}})$ for E_1 and E_- locate at the border between the blue and yellow regions, and the critical curve $\theta(\lambda_{TI_{27}})$ for E_2 locates at the border between the blue and green regions.

6. Discussion

Immune checkpoint inhibitors such as anti-PD-1 and anti-PD-L1 have been using in combination with other drugs in the cancer treatment to restore the immune responses and improve the treatment efficacy. The cytokine IL-27 has both anti-tumor and pro-tumor activities, such that its functions in cancer treatment are controversial. In this work, we had created a simplified ODE model (2.5) for the combination treatment of anti-PD-1 and IL-27 to investigate the questions: (i) To what degree anti-PD-1 improves the efficacy of IL-27, and (ii) Whether IL-27 is pro-tumor or anti-tumor in the combination with anti-PD-1.

In our simulation, we first mimicked the experimental results of tumor volume in melanoma presented in [38], by taking the same dose of IL-27 used in their experiment (i.e., $I_{27} = f_0 = 1.1 \times 10^{-6}$ g/cm^3). Our results showed that, at a small treatment efficacy of anti-PD-1, the anti-PD-1 monotherapy only reduced tumor cell density slightly, the IL-27 monotherapy had a significant reduction of tumor cell density, and the highest tumor cell density reduction appeared in the combination of IL-27 and anti-PD-1. This result qualitatively agrees with the experimental data presented in [38] that IL-27 inhibits tumor growth at selected dose of IL-27. Since IL-27 could induce a larger amount of PD-1-PD-L1, we hypothesized that IL-27 could switch to pro-tumor at a larger dosage. Thus, we increased the dose of IL-27 to $5f_0$ and then obtained opposite treatment outcome that the IL-27 monotherapy led to a significant increase of tumor cell density, even though combining IL-27 and anti-PD-1 reduced the tumor cell density slightly. This result supports our hypothesis that a larger dose of IL-27 could lead to tumor promotion.

Next, we performed the synergy analysis with the IL-27 dosage $0 \leq I_{27} \leq 5f_0$ and the treatment efficacy of anti-PD-1 $0 \leq G \leq 0.4$ (namely, the efficacy of anti-PD-1 was varying from small to moderate) to further investigate the efficacy of the combination treatment of IL-27 and anti-PD-1. Our result showed that:

(i) Increasing G increased the reduction of tumor cell density regardless of the dosage of IL-27. This result provided the degree of anti-PD-1 for improving the efficacy of IL-27.

(ii) There existed a monotone increasing curve, $F_c(G)$ depending on G, that distinguished the functions of IL-27 based on its dosage.

(ii-a) Under a small dosage of IL-27 (i.e., $I_{27} < F_c(G)$), the anti-PD-1 efficiently (indirectly) reduced the amount of PD-1-PD-L1, such that the increased activated T cells by IL-27 efficiently killed tumor cells resulting in tumor reduction. Thus, IL-27 acted like an anti-tumor agent in this regime.

(ii-b) Under a high dosage of IL-27 (i.e., $I_{27} > F_c(G)$), the PD-1-PD-1 was significantly increased by IL-27 such that the same amount of anti-PD-1 could not efficiently reduce the amount of PD-1-PD-L1. Thus, T cells were still deactivated by a large amount of PD-1-PD-L1 and hence could not efficiently kill tumor cells resulting in tumor promotion. Thus, IL-27 acted like a pro-tumor agent in this regime. Therefore, this finding addresses whether IL-27 is pro-tumor or anti-tumor in the combination with anti-PD-1.

We also analyzed the basic dynamics of the model (2.5) to obtain the existence and the local stability of the trivial, non-negative, and positive equilibria. We then provided a numerical example to study the effect of the IL-27 dosage on the equilibria. Our results showed that, in the presence of IL-27, tumor cells could not be eliminated and T cells and IFN-γ vanished, when the production rate of T cells by IL-27 was relatively small or the concentration of IL-27 was low.

Our finding provides a method to clarify the controversy of IL-27 by showing the critical curve $F_c(G)$ that separates the dosage of IL-27 for treatment efficacy, in the combination with anti-PD-1. Therefore, the critical curve $F_c(G)$ could be used to determine the optimal dosages of IL-27 and anti-PD-1 that achieve the highest tumor reduction.

Our model (2.5) is highly simplified that it only includes the variables for tumor cells, T cells, and pro-inflammatory cytokine (IFN-γ), and the model neglects the following factors:

(i) The detailed dynamics of the PD-1, PD-L1, and anti-PD-1: We only consider the (indirect) variation of PD-1-PD-L1 by IL-27 to focus on the functions of IL-27, so we neglect the variations of PD-1 and PD-L1 by T cells and cancer cells. Similarly, we only incorporate the (indirect) reduction of PD-1-PD-L1 by anti-PD-1, instead of considering the (direct) reduction of free PD-1 by anti-PD-1.

(ii) Different subgroups of T cells, including Th1, CD8$^+$ T cells, and regulatory T cells (T$_{reg}$s): Since T$_{reg}$s produce anti-inflammatory cytokine TGF-β and promotes tumor growth, the T cells in our model only include Th1 and CD8$^+$ T cells that produce pro-inflammatory cytokines and kill cancer cells.

(iii) The reaction between T cells and other cytokines, such as IL-2 and TGF-β: IL-27 inhibits the production of IL-2 secreted by Th1 and CD8$^+$ T cells, and the reduced IL-2 suppresses the development of Th1 and CD8$^+$ T cells and T$_{reg}$s. The reduced T$_{reg}$s then suppresses the production of TGF-β. Therefore, including these reactions increases the complexity of the model and disguises the major functions of IL-27 in tumor growth, so we exclude these cytokines and their interaction with T cells in this model.

(iv) The spatial information of cells and cytokines: For simplicity, we assumed the homogeneity of cells and cytokines in the TME and only consider the variations of cell density and cytokine concentration over time.

(v) The anti-inflammatory functions of IFN-γ: The IFN-γ is another common immunoregulatory cytokines that has both pro- and anti-inflammatory functions in the TME. For instance, the pro-inflammatory functions of IFN-γ includes promoting the recognitions of cancer cells, proliferation of CD8$^+$ T cell and cytotoxic T cells, and the activation of Th1 cells [26]. On the other hand, the anti-inflammatory functions of IFN-γ includes improving the expression of PD-L1 on T cells and cancer cells, apoptosis of Th1 cells, survival of tumor cells, and reducing the killing rates of cancer cells by Th1 cells and CD8$^+$ T cells [26]. Therefore, the interaction of the pro- and anti-inflammatory functions of IFN-γ and IL-27 in tumor growth is intricate. In order to clarify the main functions of IL-27, we only include the major pro- and anti-inflammatory functions of IL-27 and only incorporate the pro-inflammatory function of IFN-γ.

In [13], we created a free boundary PDE model incorporating the factors (i)-(iv) to investigate the tumor growth under the IL-27 and anti-PD-1 combination treatment. The complicated model in [13] displays a similar dynamics to the model (2.5) that IL-27 is anti-tumor at a small dosage and pro-tumor at a large dosage, as well as anti-PD-1 improves the treatment efficacy of IL-27. This comparison indicates that excluding the detailed factors (i)-(iv) does not dramatically change the dynamics of tumor growth, even though the factors (i)-(iv) provide more information and more accurate model predictions. On the other hand, in [26], we created another free boundary PDE model incorporating the factor (v) to investigate the treatment efficacy of IFN-γ and anti-PD-1. Our numerical results in [26] suggest that whether IFN-γ is an anti-tumor agent or pro-tumor agent highly depends on the cancer type. The complexity of the models in [13, 26] provides a better model prediction, but limits the mathematical analysis and disguises the major functions of IL-27. Thus, the main goal of this work is to create a simple ODE model to investigate how the activation of T cells (i.e., the major pro-inflammatory function) and up-regulation of PD-1 and PD-L1 (i.e., the major anti-inflammatory function) by IL-27 affect the tumor growth. Additionally, the simplicity of the model allows us performing mathematical analysis to further investigate the properties of the model and dynamics of tumor growth under the effect of IL-27. Our conclusions provide the preliminary study of the combination of IL-27 and anti-PD-1

in cancer treatment. These findings need to be validated experimentally and clinically, and an extended model with some missing information and feasibility of analysis is required for further investigation.

Acknowledgements

Methods

Parameter Estimation. Estimation of steady states.

We take the steady state of C to be 0.4965 g/cm^3 from the rhabdomyosarcoma model in [11], when there is no IL-27. Fig. 5A in [28] shows that the tumor volume in plasmacytoma is around 80 mm^3 in the presence of IL-27 and the tumor volume in plasmacytoma is around 336 mm^3 in the absence of IL-27, and hence the IL-27 reduces the plasmacytoma tumor volume by a factor of 0.24. Thus, we set the steady state of C to be 0.1192 g/cm^3 in the presence of IL-27.

The steady state of T is set to be 1×10^{-3} g/cm^3 in the absence of IL-27 in the rhabdomyosarcoma model [11]. Moreover, Fig. 3A in [38] shows that, in melanoma, the percentage of CD8$^+$ T cells is 3.5% in the absence of IL-27 and is 8.6% in the presence of IL-27, so IL-27 increases the percentage of CD8$^+$ T cells by a factor of 2.5 in melanoma. Thus, we take the steady state of T in the presence of IL-27 to be 2.5 fold of the steady state of T in the absence of IL-27, i.e., $T^* = 2.5 \times 10^{-3}$ g/cm^3 in the presence of IL-27.

We take the steady state of IFN-γ to be 4.5×10^{-11} g/cm^3 from the data in B16 melanoma (Fig. 4B in [21]). Moreover, in plasmacytoma (Fig. 3D in [28]), the concentration of IFN-γ has around 56% reduction (namely, reduces from 3155.8 pg/ml to 1399.7 pg/ml) in the presence of IL-27. Thus, we set the steady state of IFN-γ to be 2×10^{-11} g/cm^3 in the presence of IL-27. We also take the steady state of IL-27 to be $I_{27}^* = 1.1 \times 10^{-6}$ g/cm^3 from the melanoma data (Fig. 1A in [38]).

In summary, in the absence of IL-27 (i.e., the wild type tumor or control case, the steady states of all variables are as follows

$$C^* = 0.4965 \ g/cm^3, \ T^* = 1 \times 10^{-3} \ g/cm^3, \ I_\gamma^* = 4.5 \times 10^{-11} \ g/cm^3, \tag{6.1}$$

while in the presence of IL-27 the steady states of all variables are as follows

$$C_+^* = 0.1192 \ g/cm^3, \ T_+^* = 2.5 \times 10^{-3} \ g/cm^3, \ I_{\gamma,+}^* = 2 \times 10^{-11} \ g/cm^3, \ I_{27}^* = 1.1 \times 10^{-6} \ g/cm^3. \tag{6.2}$$

Estimation of half-saturation parameters k_X.

We set the half-saturation parameters k_X to be the steady state of X such that $X/(k_X + X) = 0.5$ while X approaching X^*, in the absence of IL-27 (i.e., the control case). Thus,

$$k_C = C^* = 0.4965 \ g/cm^3, k_\gamma = I_\gamma^* = 4.5 \times 10^{-11} \ g/cm^3.$$

For simplicity, we take k_{27} and k_q to be the steady state of IL-27, so

$$k_{27} = k_q = 1.1 \times 10^{-6} \ g/cm^3.$$

Estimation of parameters in $Q(I_{27})$.

In Eq. (2.2), when there is no anti-PD-1 (i.e., $G = 0$), we assume that the amount of PD-1-PD-L1 is relatively low in the absence of IL-27 and take

$$Q_0 = 0.01. \tag{6.3}$$

We also assume that the reduction of T cells by PD-1-PD-L1 is around 20% when IL-27 approaches its steady state and there is no anti-PD-1, i.e.,

$$\frac{1}{1 + Q(I_{27}^*) \times (1 - G)} = 4/5, \text{ with } G = 0. \tag{6.4}$$

Thus, we obtain $Q(I_{27}^*) = 0.25$ and $V_{max} = 0.24$.

Estimation of parameters in Eq. (2.1).
Fig. 7D in [38] shows that the melanoma tumor volume in the control case doubles in 3 days (611 mm^3 at time $t = 16 \ days$ and 1136 mm^3 at time $t = 19 \ days$), so we use the exponential growth equation

$$\frac{dC}{dt} = \lambda_0 C$$

to estimate the growth rate $\lambda_0 = ln2/3days = 0.231/day$.

In the absence of IL-27, the steady state of Eq. (2.1) leads to

$$\lambda_C C^* \left(1 - \frac{C^*}{C_M}\right) - \eta_C T^* C^* - \mu_C C^* = \lambda_0 C^*, \tag{6.5}$$

with $\mu_C = 0.173/day$ from melanoma [25] and $C_M = 0.9 \ g/cm^3$ from breast cancer [9]. Next, we assume the tumor growth rate is doubled without immune response, namely,

$$\lambda_C C^* \left(1 - \frac{C^*}{C_M}\right) - \mu_C C^* = 2\lambda_0 C^*, \tag{6.6}$$

so we have

$$\lambda_C = \frac{2\lambda_0 + \mu_C}{(1 - C^*/C_M)} = 1.416/day.$$

From Eqs. (6.5) and (6.6), we have $\lambda_0 C^* = \eta_C T^* C^*$ and hence $\eta_C = \lambda_0/T^* = 231 \ cm^3/g/day$.

Estimation of parameters in Eq. (2.2).
We consider the case without IL-27 and anti-PD-1 (i.e., $I_{27} = G = 0$) to simplify the steady state of Eq. (2.2) to

$$\left(\lambda_{TC} T^* \frac{C^*}{k_C + C^*} + \lambda_{TI_\gamma} T^* \frac{I_\gamma^*}{I_\gamma^* + k_\gamma}\right) \times \frac{1}{1 + Q_0} = \mu_T T^*,$$

with $Q_0 = 0.01$ due to Eq. (6.3). Since T cells (namely, Th1 and CD8$^+$ T cells) are mainly induced by IFN-γ [8, 29], we assume $\lambda_{TC} = \lambda_{TI_\gamma}/100$ and obtain

$$\left(\frac{\lambda_{TI_\gamma}}{100} T^* \times 0.5 + \lambda_{TI_\gamma} T^* \times 0.5\right) \times 0.9901 = \mu_T T^*$$

with $\mu_T = 0.3/day$ from melanoma [25]. Thus, we have $\lambda_{TI_\gamma} = 0.6/day$ and $\lambda_{TC} = 0.006/day$.

Next, we consider the case with IL-27 and take the steady state from Eq. (6.2) to estimate $\lambda_{TI_{27}}$. By using the assumption in Eq. (6.4), the steady state of Eq. (2.2) in the presence of IL-27 is

$$\left(\lambda_{TC} T_+^* \frac{C_+^*}{C_+^* + k_C} + \lambda_{TI_\gamma} T_+^* \times \frac{I_{\gamma,+}^*}{I_{\gamma,+}^* + k_\gamma} + \lambda_{TI_{27}} T_+^* \times \frac{I_{27}^*}{I_{27}^* + k_{27}}\right) \times \frac{4}{5}$$

$$= \left(0.1936\lambda_{TC} T_+^* + 0.3077\lambda_{TI_\gamma} T_+^* + 0.5\lambda_{TI_{27}} T_+^*\right) \times \frac{4}{5}$$

$$= \mu_T T_+^*,$$

due to $C_+^*/(C_+^* + k_C) = 0.1936$, $I_{\gamma,+}^*/(I_{\gamma,+}^* + k_\gamma) = 0.3077$, and $I_{27}^*/(I_{27}^* + k_{27}) = 0.5$. Thus,

$$\lambda_{TI_{27}} = 2(1.25\mu_T - 0.1936\lambda_{TC} - 0.3077\lambda_{TI_\gamma}) = 0.1756/day.$$

Estimation of parameters in Eq. (2.4)**.**
When there is no IL-27, the steady state of Eq. (2.4) is

$$0 = \lambda_{I_\gamma T} T^* - \mu_\gamma I_\gamma^*.$$

Since the half-life of IFN-γ is about 4.5 hours [2], we take

$$\mu_\gamma = \frac{\ln 2}{(4.5/24)\text{day}} = 3.68/\text{day}.$$

Thus, we have $\lambda_{I_\gamma T} = \mu_\gamma I_\gamma^*/T^* = 1.656 \times 10^{-7}/\text{day}$.

When IL-27 is administered and approaches to its steady state I_{27}^*, we assume that IL-27 reduces IFN-γ production by T cells by 20%, i.e.,$s_\gamma/(I_{27}^* + s_\gamma) = 4/5$, to obtain $s_\gamma = 4I_{27}^* = 4.4 \times 10^{-6} \ g/cm^3$.

REFERENCES

[1] M. Ando, Y. Takahashi, T. Yamashita, M. Fujimoto, M. Nishikawa, Y. Watanabe et al., *IFN-γ from lymphocytes induces PD-L1 expression and promotes progression of ovarian cancer*, Br J Cancer. **112**(2015), 1501-1509.

[2] M. Ando, Y. Takahashi, T. Yamashita, M. Fujimoto, M. Nishikawa, Y. Watanabe, Y. Takakura, *Prevention of adverse events of interferon γ gene therapy by gene delivery of interferon-γ-heparin-binding domain fusion protein in mice*, Mol Ther Methods Clin Dev. **1**(2014): 14023.

[3] D. Bortz, P. Nelson, *Sensitivity analysis of a nonlinear lumped parameter model of HIV infection dynamics*, Bull Math Biol. **66**(2004), 1009–1026.

[4] O. Boyman, J.H. Cho, J. Sprent, *The role of interleukin-2 in memory CD8 cell differentiation*, Adv Exp Med Biol. **684**(2010), 28-41.

[5] G. Carbotti, G. Barisione, I. Airoldi, D. Mezzanzanica, M. Bagnoli, S. Ferrero et al. *IL-27 induces the expression of IDO and PD-L1 in human cancer cells*, Oncotarget. **6**(2015), 43267-43280.

[6] F. Castro, A.P. Cardoso, R.M. Goncalves, K. Serre, M.J. Oliverira, *Interferon-gamma at the crossroads of tumor immune surveillance or evasion*, Front Immunol. **9**(2018): 847.

[7] C. Cocco, N. Giuliani, E. Di Carlo, E. Ognio, P. Storti, M. Abeltino et al. *Interleukin-27 acts as multifunctional antitumor agent in multiple myeloma*, Clin Cancer Res. **16**(2010), 4188-4197.

[8] J.M. Curtsinger, P. Agarwal, D.C. Lins, M.F. Mescher, *Autocrine IFN-γ promotes native CD8 T cell differentiation and synergizes with IFN-α to stimulate strong function*, J. Immunol. **189**(2012), 659-668.

[9] T.D. Eubank, R.D. Roberts, M. Khan, J.M. Curry, G.J. Nuovo, P. Kuppusamy et al. *Granulocyte macrophage colony-stimulating factor inhibits breast growth and metastasis by invoking an anti-angiogenic program in tumor educated macrophages*, Cancer Res. **69**(2009), 2133–2140.

[10] M. Fabbi, G. Carbotti, S. Ferrini, *Dual roles of IL-27 in cancer biology and immunotherapy*, **2017**(2017): 3958069.

[11] A. Friedman, X. Lai, *Combination therapy for cancer with oncolytic virus and checkpoint inhibitor: A mathematical model*, PLoS One. **13**(2018), e0192449.

[12] A. Friedman, K.-L. Liao, *The role of the cytokines IL-27 and IL-35 in cancer*, Mathematical Biosciences and Engineering, **12**(2015), 1203-1217.

[13] K.-L. Liao, X.-F. Bai, A. Friedman, *IL-27 in combination with anti-PD-1 can be anti-cancer or pro-cancer agent*, prepare for submission, 2022.

[14] J. Gonin, A. Carlotti, C. Dietrich, A. Audebourg, B. Radenen-Bussiere, A. Caignard et al *Expression of IL-27 by Tumor Cells in InvasCutaneous and Metastatic Melanomas*, PLoS One. **8**(2013): e75694.

[15] J. Guan, K.S. Lim, T. Mekhail, C.C. Chang, *Programmed death ligand-1 (PD-L1) expression in the programmed death receptor-1 (PD-1)/PD-L1 blockade: a key player against various cancers*, Arch Pathol Lab Med. **141**(2017): 851-861.

[16] K. Hirahara, K. Ghoreschi, X.P. Yang, H. Takahashi, A. Laurence, G. Vahedi et al. *Interleukin-27 priming of T cells controls IL-17 production in trans via induction of the ligand PD-L1*, Immunity. **36**(2012), 1017-1030.

[17] M. Huber, V. Steinwald, A. Guralnik, A. Brustle, P. Kleemann, C. Rosenplanter, et al *IL-27 inhibits the development of regulatory T cells via STAT3*, Int Immunol. **20**(2008), 223-234.

[18] C.A. Hunter, *New IL-12-family members: IL-23 and IL-27, cytokines with divergent functions*, Nat Rev Immunol. **5**(2005), 521-531.

[19] C.A. Hunter, R. Kastelein, *Interleukin-27: balancing protective and pathological immunity*, Immunity. **37**(2012), 960-969.

[20] E.S. Hwang, J.-H. Hong, L.H. Glimcher, *IL-2 production in developing Th1 cells is regulated by heterodimerization of RelA and T-bet and requires T-bet serine residue 508*, JEM. **202**(2005), 1289-1300.

[21] S. Ishikawa, T. Ishikawa, C. Tezuka, K. Asano, M. Sunagawa, T. Hisamitsu, *Efficacy of juzentaihoto for tumor immunotherapy in B16 melanoma metastasis model*, Evid Based Complement Alternat Med. **2017** (2017): 6054706.

[22] X. Lai, A. Friedman, *Combination therapy of cancer with cancer vaccine and immune checkpoint inhibitors: A mathematical model*, PLoS One. **12**(2017): e0178479.

[23] X. Lai, A. Friedman, *Combination therapy for melanoma with BRAF/MEK inhibitor and immune checkpoint inhibitor: a mathematical model*, BMC Syst Biol. **11**(2017): 70.

[24] X. Lai, A. Friedman, *Mathematical modeling of cancer treatment with radiation and PD-L1 inhibitor*, Science China Mathematics. **63**(2020), 465-484.

[25] K.-L. Liao, X.-F. Bai, A. Friedman, *Mathematical modeling of Interleukin-27 induction of anti-tumor T cells response*, PLoS ONE, **9**(2014): e91844.

[26] K.-L. Liao, K.D. Watt, *Mathematical modeling and analysis of anti-PD-1 and IFN-gamma synergy in cancer immunotherapy*, Mathematical Biosciences, **353**(2022): 108911.

[27] J. Liu, Z. Chen, Y. Li, W. Zhao, J. Wu, Z. Zhan, *PD-1/PD-L1 checkpoint inhibitors in tumor immunotherapy*, Frontiers in Pharmacology, **12**(2021): 2339.

[28] Z. Liu, J.-Q. Liu, F. Talebian, L.-C. Wu, S. Li, X.-F. Bai, *IL-27 enhances the survival of tumor antigen-specific CD8$^+$ T cells and programs them into IL-10-producing, memory precursor-like effector cells*, Eur. J. Immunol. **43**(2013), 468-479.

[29] R.V. Luckheeram, R. Zhou, A.D. Verma, B. Xia, *CD4$^+$ T cells: differentiation and functions*, Clin Dev Immunol. **2012**(2012): 925135.

[30] S. Marino, I.B. Hogue, C.J. Ray, D.E. Kirschner, *A methodology for performing global uncertainty and sensitivity analysis in systems biology*, J Theor Biol. **254**(2008), 178-196.

[31] M. Masahiro, K. Tsunao, N. Hiroshi, Y. Koichiro, S.-Y. Masaharu, S. Taketoshi et al. *Interleukin-27 activates natural killer cells and suppresses NK-resistant head and neck squamous cell carcinoma through inducing antibody-dependent cellular cytoxicity*, Cancer Res. **69**(2009), 2523-2530.

[32] M.A. Postow, M.K. Callahan, J.D. Wolchok, *Immune checkpoint blockade in cancer therapy*, J Clin Oncol. **33**(2015), 1974-1982.

[33] R. Salcedo, J.K. Stauffer, E. Lincoln, T.C. Back, J.A. Hixon, C. Hahn et al. *IL-27 mediates complete regression of orthotopic primary and metastatic murine neuroblastoma tumors: role for CD8$^+$ T cells*, J Immunol. **173**(2004), 7170-7182.

[34] A.H. Sharpe, K.E. Pauken, *The diverse functions of the PD1 inhibitory pathway*, Nat Rev Immunol. **18**(2018), 153-167.

[35] L. Shi, S. Chen, L. Yan, Y. Li, *The role of PD-1 and PD-L1 in T-cell immune suppression in patients with hematological malignancies*, J Hematol Oncol. **6**(2013): 74.

[36] M. Swart, I. Verbrugge, J.B. Beltman, *Combination approaches with immune-checkpoint blockade in cancer therapy*, Front Oncol. **6**(2016): 233.

[37] E.D. Wojno, N. Hosken, J.S. Stumhofer, A.C. O'Hara, E. Mauldin, Q. Fang et al. *A role for IL-27 in limiting T regulatory cell populations*, J Immunol. **187**(2011), 266-273.

[38] J. Zhu, J.Q. Liu, M. Shi, X. Cheng, M. Ding, J.C. Zhang, et al. *IL-27 gene therapy induces depletion of Tregs and enhances the efficacy of cancer immunotherapy*, JCI Insight. **3**(2018): e98745.

[39] W. Zou, J.D. Wolchok, L. Chen, *PD-L1 (B7-H1) and PD-1 pathway blockade for cancer therapy: mechanisms, response biomarkers and combinations*, Sci Transl Med. **8**(2016): 328rv4.

Department of Mathematics, University of Manitoba, Winnipeg, Manitoba, R3T 2N2, Canada
Email address: wattk2@myumanitoba.ca

Corresponding author, Department of Mathematics, University of Manitoba, Winnipeg, Manitoba, R3T 2N2, Canada
Email address: Kang-Ling.Liao@umanitoba.ca